Multi-objective Optimization of Industrial FCC Units using *Elitist* Non-dominated Sorting Genetic Algorithm

A Thesis Submitted
in Partial Fulfilment of the Requirements
for the Degree of
MASTER OF TECHNOLOGY

by

Rahul B. Kasat

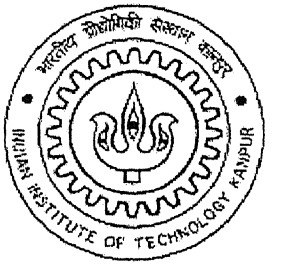

to the

Department of Chemical Engineering

INDIAN INSTITUTE OF TECHNOLOGY, KANPUR

January 2002

CERTIFICATE

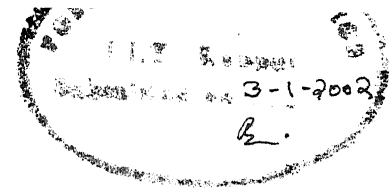

This is to certify that the work contained in the thesis entitled 'MULTI-OBJECTIVE OPTIMIZATION OF INDUSTRIAL FCC UNITS USING *ELITIST* NON-DOMINATED SORTING GENETIC ALGORITHM', has been carried out by Mr. Rahul B. Kasat, under our supervision and has not been submitted elsewhere for a degree.

Dr. D. N. Saraf

Department of Chemical Engineering,
Indian Institute of Technology,
Kanpur-208016
India.

Dr. Santosh K. Gupta

Department of Chemical Engineering,
Indian Institute of Technology,
Kanpur-208016
India.

January, 2002

Acknowledgement

Very few people have got this 'opportunity' till date and I consider myself lucky enough to be one of them. Getting a combined guidance from Prof. Santosh K. Gupta, Prof. D. N. Saraf and Prof. D. Kunzru was one of the best things happened to me at IIT Kanpur.

First of all I express my deep sense of gratitude to Prof. Santosh K. Gupta for his constant encouragement throughout my stay at IIT Kanpur. He taught me how to think rather than what to think. I have never seen a perfectionist like him. The words 'thank you' are insufficient if I recall each and every thing I have learnt from him.

I would like to thank Prof D. N. Saraf for his constant help during the completion of the thesis work. He was always there for discussion whenever I needed him during my thesis work. I would like to thank Prof. D. Kunzru for his valuable comments during the critical stages. The valuable information I used to get during my meetings with all of them, I am sure, cannot be obtained from any written source.

I would like to thank Dhaval Dave for providing me simulation code and also helping me out in the early stages of my thesis. I would also like to thank my lab mates, Tejas, Swarnendu, Anjana, Sameer and Arpan for their co-operation. They never argued with me whenever I needed PC for thesis work. I would also like to thank Ashutosh and Ved (Saraf sir's lab students) who cooperated with me while running my computer codes on their PCs.

How can I forget my two buddies 'Shrikant and Sunil'? They were always there in all ups and downs (especially on the dinner table). I would also like to say thanks to Rupali. She was always there in the crisis time (especially while drawing 3D graphs in gnuplots). I would like to thank Pawan and Ganesh with whom I had discussed whole lot of issues. All these people were always there whenever I needed them and so they own special thanks again.

I would also like to thank my school friends (spcricket egroup) and my B.Tech. friends (chemenglit egroup) who kept on sending lot of emails to my account and kept on pushing me for doing a good work.

I would also like to thank Shubhra auntie for all kinds of delicious sweets, namakins, and also tomato soup during my discussion with Gupta sir at his residence on holidays (especially Sunday mornings) and also in the last few weeks of submission.

This acknowledgement will be incomplete if I fail to remember my parents. They are always a source of inspiration for me and always support me in all the decisions I have taken in my life. I would like to thank to my sister Rakhi and my Jijaji for their constant support. I would also like to thank Rashmi who is very close to my heart and who kept on asking me when I would complete my project and come back to Pune.

Finally I would like to thank DST for providing the financial support during the completion of this work.

Contents

List of Figures

List of Tables

Nomenclature

A	cross-sectional area of regenerator, ft^2
A_{rgn}	cross-sectional area of regenerator, m^2
A_{ris}	cross-sectional area of riser, m^2
C_c	coke on catalyst at any location, (kg coke)(kg catalyst)$^{-1}$
C_i	concentration of i^{th} lump, kmol m^{-3}
C_H	weight fraction of H_2 in coke, (kg H_2)(kg coke)$^{-1}$ (Table 3)
C_{rgc}	coke on regenerated catalyst, (kg coke)(kg cat)$^{-1}$
C_{sc}	coke on spent catalyst, (kg coke)(kg cat)$^{-1}$
Cp_c	heat capacity of catalyst, kJ kg^{-1} K^{-1}
Cp_{f_l}	heat capacity of liquid feed, kJ kg^{-1} K^{-1}
Cp_{f_v}	heat capacity of vapor feed, kJ kg^{-1} K^{-1}
Cp_i	mean heat capacity of i [H_2O, N_2, O_2], kJ kg^{-1} K^{-1}
Cp_{tot}	heat capacity of (total) mixture, kJ kg^{-1} K^{-1}
D	diameter of regenerator, ft
D_p	average diameter of catalyst particle, ft
E_c, E_β	activation energies, kJ kmol^{-1}
E_i	activation energy of i^{th} reaction, kJ kmol^{-1}
f_i	molar flow rate of i [CO, CO_2, H_2O, N_2, O_2, carbon] in the regenerator, kmol s^{-1}
f_{tot}	total gas flow rate at any location in the regenerator, kmol s^{-1}
F_{air}	flow rate of air feed to the regenerator, kmol s^{-1}
F_{ent}	entrained catalyst flow rate, kg s^{-1}

F_{feed}	feed flow rate of oil, kg s^{-1}
F_j	molar flow rate of j^{th} lump, kmol s^{-1}
F_{rgc}	flow rate of regenerated catalyst, kg s^{-1}
F_{sc}	flow rate of spent catalyst, kg s^{-1}
g	gravitational acceleration, 32.2 ft sec^{-2}
h	dimensionless height of riser ($\equiv z/H_{ris}$)
ΔH_{evp}	heat of vaporization of gas oil feed, kJ kg^{-1}
H_i	heat of formation of i, kJ $kmol^{-1}$
ΔH_i	heat of i^{th} reaction, kJ $kmol^{-1}$
H_{ris}	height of riser, m
$k_{0,i}$	frequency factor for i^{th} reaction (Tables 1, 2)
k_c	overall rate of combustion of coke
k_i	reaction rate constant for i^{th} reaction (Tables 1, 2)
MW_c	molecular weight of coke, kg $kmol^{-1}$
MW_g	average molecular weight of gas phase, kg $kmol^{-1}$
MW_j	molecular weight of j^{th} lump, j = 1, 2, ..., 5, kg $kmol^{-1}$
MW_H	molecular weight of H_2, kg $kmol^{-1}$
P_{rgn}	pressure in regenerator, atm
P_{ris}	pressure in riser, atm
r_i	rate of the i^{th} reaction, i=1 to 9 (riser); i = 10 to 12 (regenerator), kmol (kg catalyst)$^{-1}$ s^{-1} or kmol $m^{-3}s^{-1}$
R	universal gas constant, J K^{-1} $kmol^{-1}$
T_{air}	temperature of air fed to the regenerator, K
T_{base}	base temperature for heat balance calculations, K (assumed, 866.6 K)

T_{dil} temperature of dilute phase at any location, K

T_{feed} temperature of gas oil feed, K

T_{rgn} temperature (uniform) of dense bed, K

T_{ris} temperature of riser at any location, K

$T_{ris,top}$ temperature at top of riser, K

T_{sc} temperature of spent catalyst [$= T_{ris,top} - \Delta T_{st}$], K

ΔT_{st} temperature drop in stripper (assumed 10 K)

u velocity of gas in the riser or the regenerator, m s^{-1}

u_1 superficial linear velocity, ft s^{-1}

W catalyst entrainment flux, lb (ft^2 regenerator area)$^{-1}$ s^{-1}

x_j mole fraction of j^{th} lump, j = 1, 2, ..., 5

x_{pt} relative (catalytic) CO combustion rate (Eq. A 16)

Y (kg catalyst entrained in dilute phase) (kg fluidizing vapor)$^{-1}$

z height from the entrance of the regenerator, m

Z_{bed} height of the dense bed, m

Z_{dil} height of the dilute phase, m

Z_{rgn} total height of the regenerator, m

Greek

α_{ij} stoichiometric coefficient of j^{th} species in i^{th} reaction, based on mass

β_c CO/CO_2 ratio at catalyst surface in regenerator (Table 2)

ε void fraction in riser or regenerator at any location

ε_{dil} void fraction in the dilute phase at any location

ρ_c density of solid catalyst (not including void fraction), kg m^{-3}

ρ_{dil}	density of catalyst in the dilute phase, kg m^{-3}
ρ_f	density of fluidization vapor, lb ft^{-3}
ρ_g	density of gas phase in the regenerator, kmol m^{-3}
ρ_p	density of catalyst particle (solid), lb ft^{-3}
ρ_v	density of vapor at any location, kg m^{-3}
ϕ	activity of the catalyst

Subscripts

i, j	i^{th} or j^{th} lump; 1: gas oil, 2: gasoline, 3: LPG, 4: dry gas, 5: coke

ABSTRACT

This study provides insights into the optimal operation of one of the most important refinery units, namely, the fluidized-bed catalytic cracking unit (FCCU). A five-lump model is used to characterize the feed and the products. The model is first tuned using some industrial data. An *elitist* non-dominated sorting genetic algorithm (NSGA-II) is used to solve a few meaningful multi-objective function optimization problems. It is observed that the non-dominating Pareto set of optimal solutions can be broadly classified into two regions: the partial-combustion and the full-combustion problems. A three-objective function optimization problem is solved. The objective functions used are: maximization of the gasoline yield, minimization of the air flow rate and minimization of the percent CO in the flue gas. The flow rate of the gas oil feed to the industrial FCCU is taken as 29 kg/s. The decision variables and several important state variables corresponding to the optimal conditions of *operation*, are obtained. The procedure used is quite general and can be applied to other industrial FCC units. The optimal results obtained here provide physical insights that can help one in obtaining and interpreting such solutions.

CHAPTER 1

INTRODUCTION

Increase in the demand for gasoline, LPG and diesel over the last several decades have led to major improvements in refinery operations. The fluidized-bed catalytic cracking unit (FCCU) is an important conversion unit in most integrated refineries. Several studies have been reported in the open literature that deal with various aspects of FCCU. These include their modeling, simulation, kinetics, on-line optimization and control. Avidan and Shinnar[1] reviewed the developments and commercialization of catalytic cracking in detail. Different workers have discussed the kinetics[2-6] in the reactor and the regenerator and have modeled[7-9] these units separately, while a few[10-16] have developed an integrated model for the reactor-regenerator system.

In case of the reactor, various models are available that describe the feed and the products in terms of different kinetic 'lumps'. These include describing the products in terms of two[17], three[2], four[18] or five[5,6] lumps, while considering the feed as a single lump. Researchers[19-21] have obtained some useful results using these models. The need to evaluate the dry gas, LPG, and the gasoline yields led to an increase in the number of lumps from two to five. Jacob et al.[4] proposed a ten-lump kinetic scheme that characterizes the *feed* in terms of eight different lumps. The *product* lumps include, in addition, gasoline and (coke + gas) lumps. Cerqueira et al.[22] proposed a twelve-lump kinetic scheme with coke and gas as separate lumps. The advantage of ten- and twelve-lump kinetic schemes is that the rate constants are independent of the feed composition, but the main problem is that a relatively large number of kinetic parameters need to be evaluated using experimental or industrial data that are not easily available.

In the FCCU, the catalyst loses its activity due to the deposition of coke. Voorhies[23], Nace et al.[24] and John et al.[25] related the catalyst activity to the time-on-stream, Froment and Bischoff[26] have related this decay to the amount of coke deposited on the catalyst, while Beeckman and Froment[27] have accounted for the pore size distribution and the arrangement of the pores in the catalyst.

Several models are available in the literature for the regenerator, e.g., simple models,[7,9] grid-effect models,[8] two-region models[28,29] and the bubbling bed model.[30] Several studies[10-16,31,32] have been reported on the integrated models that include both the reactor and the regenerator. It is clear that a considerable amount of effort has been put into the modeling of FCCU. A large number of complex equations need to be solved simultaneously to obtain results numerically.

Several studies have been carried out on the optimization of FCCUs. Dynamic optimization of an FCCU was carried out by Davis et al.[33] and Webb et al.[34] Rhemann et al.[35] carried out online control and optimization of FCCUs. McFarlane and Bacon[36] used the adaptive optimizing control strategy to study the dynamic history of input/output variables with respect to changes in the ambient temperature and the 'coke factor'. They used a profit function as the objective function in their study and the regenerator temperature, reactor temperature, catalyst circulation rate and the air supply rate as the four decision (optimizing) variables. Chitnis and Corripio[37] used SMCO (supervisory multivariable constrained optimization) to optimize FCCUs. The aim of their study was to minimize the objective function that included a cost term, a constraint term and a 'move-suppression' term. They followed the study done by McFarlane and Bacon. Ellis et al.[31] used SQP (successive quadratic programming) to

study the sensitivity of the economic objective function for online optimization. They used the regenerator temperature, riser temperature, gas oil feed flow rate and stack gas oxygen concentration as the decision variables. Khandalekar and Riggs[38] used the optimization method of Nelder and Mead[39] for the inner cycle to get the regenerator and riser temperatures, and the Fibonnaci method[40] for the outer cycle to obtain the optimal feed rate. The decision variables used by Khandalekar and Riggs were the same as those used by Ellis et al. Recently, Ramasubramanian et al.[41] used the optimization procedure of Luus and Jaakola[42] to maximize a performance index defined by them. They used nine different decision variables in their study. In addition to the decision variables used in the previous studies,[31,37,38] they used the wet gas compressor valve position, reactor-regenerator pressure difference, governor set-point for lift air blower, combustion air blower suction valve position, and the spill air valve position as additional decision variables. More recently, Zhao et al.[43] used artificial neural network (ANN) and modified genetic algorithm (a modification of the conventional GA[44-46]) to optimize the operation of FCCUs. They used ANN for describing the relation between conversion ratio and the influencing factors. They found that ANN is better than available empirical models. Till now, all the optimization studies of FCCUs have used only a single objective function. In this study, however, we use an adaptation of genetic algorithm (NSGA-II), as developed by Deb and coworkers[48,55] to optimize industrial FCCUs using more than one objective function. Such studies, we believe, are more realistic. Indeed, multi-objective optimization has been carried out for several industrial units[49-56] in chemical engineering using an earlier adaptation of GA developed by Srinivas and Deb[47] (NSGA-I).

This is the first study in the field of chemical engineering in which we are using NSGA-II,[48,55] a more recent and improved version of NSGA-I,[47] to obtain solutions for the FCCU, which is well known to be a computationally intensive system. Also, this is the first attempt in the field of FCCU system optimization where more than a single objective function has been used so as to obtain more meaningful and realistic results.

Process Description

The FCCU consists of two major units, a reactor/riser and a regenerator, as shown in Figure 1. The feed to this unit, consisting mainly of heavy gas oil, vacuum gas oil or coker oil, is preheated to a temperature, T_{fccd}, and gets mixed with the hot regenerated catalyst at temperature, T_{rgn}, at the base of the riser. The feed is mixed with a small amount of steam, which helps in good atomization and reduction in coke formation by reducing the partial pressure of hydrocarbon vapors. All cracking reactions taking place in the riser are endothermic. Lighter hydrocarbons are produced in the riser. Byproduct coke is formed simultaneously which deposits on the catalyst surface and reduces the activity of the catalyst. The amount of coke formed depends upon the coking characteristics of the feedstock and also on the operating conditions. At the top of the riser, the product vapors are separated from the catalyst in the disengaging section (separator in Fig. 1) of the reactor and sent to the main fractionator for separation. The hydrocarbon left on the catalyst surface is removed using steam stripping. The stripped spent catalyst at temperature, T_{sc}, is sent to the regenerator. The catalyst is fluidized here using air at temperature, T_{air}. The hydrogen and carbon on the regenerator catalyst react with oxygen in the air, resulting in the formation of carbon

Figure 1 Schematic diagram of fluid catalytic cracking unit

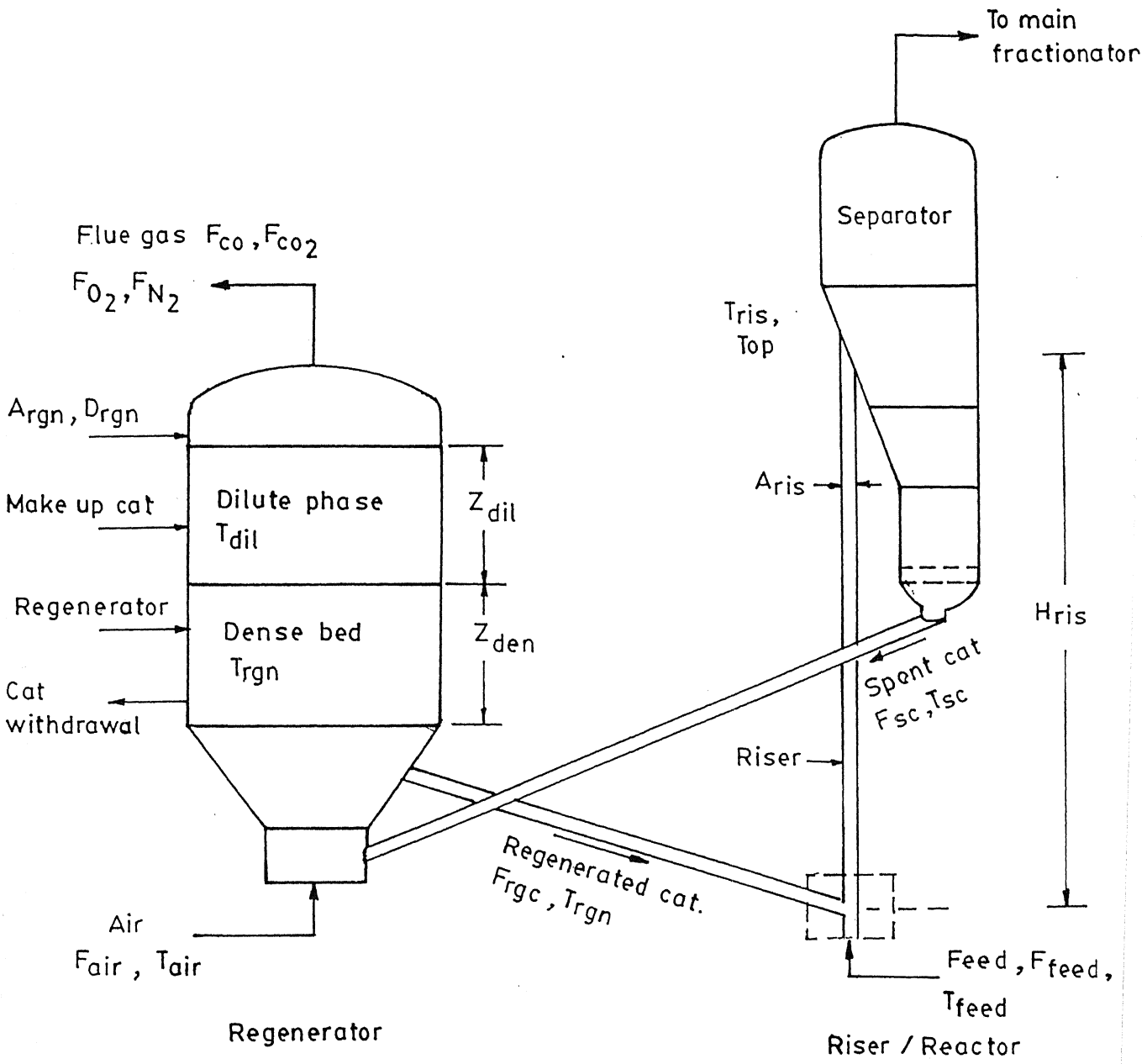

monoxide, carbon dioxide and water. The combustion reaction is exothermic. The height of the fluidized bed (dense bed) is Z_{bed}. There is a catalyst disengaging space (Z_{dil}) above the dense fluidized bed. This is referred to as the dilute bed. Entrained catalyst is finally separated from the gas in the cyclones at the top of the regenerator. The exothermic heat associated with the burning of the coke is used to keep the catalyst at high temperatures. This supplies the heat required for the vaporization and cracking of the feed in the riser. Losses in catalyst activity due to coking are temporary. However, exposure of the catalyst to high temperatures and steam can result in its permanent degradation. Attrition results in the loss of catalyst with the flue gas, and is made up for using a supply of fresh catalyst.

Model of the FCCU

In the present study, the reactor model of Dave[32] is used because of its simplicity and applicability to *industrial* units. The five-lump kinetic scheme of Ancheyta et al.[6] is used. This kinetic scheme is simple but somewhat inadequate since several of the rate constants depend on the feed composition. In contrast, the ten-lump model of Jacob et al.[4] does not suffer from this drawback, but is not used here since sufficient industrial data are not available in the open literature to 'tune' the several rate constants associated with it. Dave modified the original model of Ancheyta et al.[6] by assuming that gasoline and LPG *also* convert to coke. This modified kinetic scheme is shown in Figure 2. The rate constants and the heats of reaction are given in Table 1.[14,32,57,58]

In the study of Dave, the FCC reactor/riser has been modeled as a steady state plug flow reactor with the assumption that gas oil cracking follows second order

Figure 2 Five-lump kinetic scheme[52] used in this work

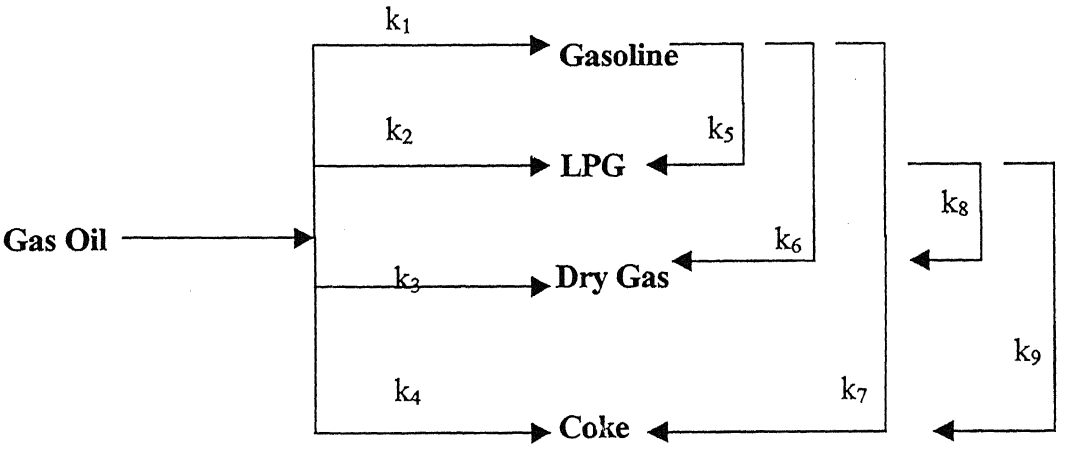

TABLE 1

Kinetic and Thermodynamic Parameters[32] used for Reactor Modeling

Rate constants	Frequency factor[*32,58]	Activation energy[57] (kJ/kmol)	Heat of reaction[14] (kJ/kmol)
k_1	14054.59[+]	57540	45000
k_2	2293.00[+]	52500	159315
k_3	390.95[+]	49560	159315
k_4	29.90[+]	31920	159315
k_5	65.40[**]	73500	42420
k_6	0.00[**]	45360	42420
k_7	0.00[**]	66780	42420
k_8	0.32[**]	39900	2100[+]
k_9	0.19[**]	31500[+]	2100[+]

* m^6 (kg catalyst)$^{-1}$(kmol gas oil)$^{-1}s^{-1}$ for k_1 - k_4

m^3(kg catalyst)$^{-1}s^{-1}$ for k_5 - k_9

+ from Ref. 32

** from Refs. 32 and 58

kinetics, while gasoline and LPG cracking reactions follow first order kinetics. The catalytic deactivation function for the cracking of vacuum gas oil is that provided by Yingxun.[59] Dave assumed the temperature drop around the stripper to be about 10 °C, and adjusted the hydrogen-to-carbon ratio in the catalyst at the entry point of the regenerator, in order to match industrial data on the regenerator temperature. The regenerator is modeled using the two-region model proposed by Krishna and Parkin[9] with some modifications.[32] Gas is assumed to be in plug flow throughout the regenerator bed and in thermal equilibrium with the surrounding solids. The catalyst is assumed to be well mixed in the dense bed and in plug flow in the dilute phase.

The main reactions taking place in the regenerator are:

$$C + \frac{1}{2}O_2 \xrightarrow{k_{10}} CO \qquad \text{(a)}$$

$$C + O_2 \xrightarrow{k_{11}} CO_2 \qquad \text{(b)}$$

$$CO + \frac{1}{2}O_2 \xrightarrow{k_{12c}} CO_2 \qquad \text{(heterogeneous CO combustion)} \quad \text{(c)}$$

$$CO + \frac{1}{2}O_2 \xrightarrow{k_{12h}} CO_2 \qquad \text{(homogeneous CO combustion)(d)} \quad (1)$$

The balance equations for O_2, CO, CO_2, as well as for H_2O (reaction not listed in Eq. 1) are given in Appendix 1. The kinetic parameters used for the regenerator model are given in Table 2.[14] The *complete* set of equations[32] are summarized in Appendix 1. Table 3 gives the thermodynamic and other parameters[32] while Table 4 gives the design details of the industrial FCCU used in this work. These are slightly modified from those corresponding to an existing industrial unit,[32] for proprietary reasons.

TABLE 2
Kinetic Parameters[14] used for Regenerator Modeling

Parameter	Frequency factor	Activation energy (E/R, K)
β_c^*	2512	6795
k_c $atm^{-1}s^{-1}$	1.0694×10^{8}	18890
k_{12c} $(kmol\ CO)(kg\ cat)^{-1}s^{-1}\ m^{-3}$	117	13890
k_{12h} $(kmol\ CO)m^{-3}atm^{-2}s^{-1}$	5.07×10^{14}	35555

$$* : \beta_c \equiv \frac{k_{10}}{k_{11}} = \beta_{c0} \exp\left[\frac{-E_\beta}{RT}\right]$$

$$k_c \equiv k_{10} + k_{11} = k_{c0} \exp\left[\frac{-E_c}{RT}\right]$$

TABLE 3

Thermodynamic and Other Parameters[32] used for Simulation

Parameter	Value
Cp_c kJ kg^{-1} K^{-1}	1.003
Cp_{f_l} kJ kg^{-1} K^{-1}	3.430
Cp_{f_v} kJ kg^{-1} K^{-1}	3.390
Cp_{N_2} kJ kg^{-1} K^{-1}	30.530
Cp_{O_2} kJ kg^{-1} K^{-1}	32.280
Cp_{H_2O} kJ kg^{-1} K^{-1}	36.932
Cp_{CO} kJ kg^{-1} K^{-1}	30.850
Cp_{CO_2} kJ kg^{-1} K^{-1}	47.400
ΔH_{evp} kJ kg^{-1}	350.0
H_{CO} kJ kmol^{-1}	1.078×10^5
H_{CO_2} kJ kmol^{-1}	3.933×10^5
H_{H_2O} kJ kmol^{-1}	2.42×10^5

TABLE 3 (contd...a)

Parameter	Value
ρ_c kg m^{-3}	1089.0
C_H (kg H_2)(kg coke)$^{-1}$	0.15
$MW_{gas\ oil}$	350
$MW_{gasoline}$	170
MW_{LPG}	65
$MW_{dry\ gas}$	30
MW_{coke}	12
$\alpha^{*}_{gas\ oil,\ gasoline}$	2.06
$\alpha_{gas\ oil,\ LPG}$	5.39
$\alpha_{gas\ oil,\ dry\ gas}$	11.67
$\alpha_{gas\ oil,\ coke}$	29.17
$\alpha_{gasoline,\ LPG}$	2.62
$\alpha_{gasoline,\ dry\ gas}$	5.67

TABLE 3 (contd...b)

Parameter	Value
$\alpha_{gasoline,\ coke}$	14.17
$\alpha_{LPG,\ dry\ gas}$	2.17
$\alpha_{LPG,\ coke}$	5.42
D_p ft	2.0×10^{-4}
x_{pt}	0.10

* : α_{ij} = for the jth lump corresponding to the reaction from lump i to lump j (in mass terms)

TABLE 4

Design Data for the FCCU Used[32] in This Study

Parameter	Value
Riser length (m)	37.0
Riser diameter (m)	0.685
Regenerator length (m)	19.4
Regenerator diameter (m)	4.5
Inventory of catalyst in regenerator (kg)	34,000.0
Feed rate (kg/s)	29.0
Riser pressure (kPa)	253.85
Regenerator pressure (kPa)	267.23

The regenerator model of the FCCU is coupled with the reactor model, and for any specified operating conditions, it can predict the product yields, coke on regenerated catalyst, temperature of the regenerated catalyst, and the flue gas composition. The Runge-Kutta-Gill method[60] is used to solve the differential equations. Guess values are assumed for the coke on regenerated catalyst, C_{rgc}, and the temperature, T_{rgn}, of the regenerated catalyst, and the equations are solved to give new values (iterates) for these two variables. Convergence is obtained using the Newton-Raphson method.[60] A tolerance of 1.5°C is used for the convergence of T_{rgn}, while a tolerance of 1×10^{-4} kg coke/kg catalyst is used in the case of C_{rgc}. It was found that sometimes the model does not converge, particularly when the decision/input variables generated by GA (that uses a random number generator for this purpose) are practically infeasible.

The model is *tuned* in order to describe the operation of the industrial FCCU more realistically. It was observed that the temperature at the base of the riser in the equation was always higher than the industrial values. Similarly, the model-predicted values of the dense bed temperature, T_{rgn}, differed slightly from industrial values. In order to minimize these two deviations, empirical heat loss terms were introduced for the riser base (dotted box shown in Fig. 1) as well as for the dense bed of the regenerator. The appropriate equations are also included in Appendix 1. Introduction of these losses led to good agreement of model-results with four sets of industrial data.[32] Results for all four sets of data are shown in Appendix II. A similar loss term was incorporated by McFarlane et al.[12] and Han et al.[15], but only for the dense bed heat balance.

Optimization

In most real life problems, one needs to optimize several (incompatible) objectives functions. This could result in a set of *several* non-dominated (equally good) Pareto-optimal[46] solutions, rather than a *unique* optimal point. The advantage of using multi-objective evolutionary techniques is that one can obtain the entire Pareto set in a *single* application of the algorithm. GA, as first developed,[44,45] has been adapted to solve multi-objective problems. One such adaptation for problems involving decision variables that are single *values*, is the non-dominated sorting genetic algorithm (NSGA-I) developed by Srinivas and Deb.[47,55] Mitra et al.[49] extended this technique to apply to problems where the decision (optimizing) variables are *functions* of time (trajectory-optimization problems). In the last few years, several studies have been reported on the multi-objective optimization of industrial units using NSGA-I. Examples in chemical engineering include the optimization of polymerization reactors,[49,50] steam reformers,[51] cyclone separators,[52] membrane separation modules,[53] etc. These have been reviewed recently by Bhaskar et al.[54] Unfortunately, NSGA-I has been observed to fail in a few cases, e.g., PET reactors,[50,56] described by a complex set of equations. A modification[48,55] of this algorithm, the *elitist* non-dominated sorting genetic algorithm (referred to, here, as NSGA-II) is now available in the literature that incorporates the concept of elitism in order to make the algorithm more powerful. Details of NSGA-II are provided in Appendix III (it is assumed that the reader is aware of the preliminary details[49] on GA and NSGA-I).

CHAPTER 2

FORMULATION

Several objective functions can be considered in any optimization study of FCCU in order to maximize its profitability and satisfy real-life constraints. In this unit, an increase in the yields of gasoline, LPG or diesel always leads to an increase in the profit. So, it is clear that the maximization of these yields should be taken as the objective function. Interestingly, an increase in the gasoline yield usually leads to an increase in the yield of LPG, and of dry gas, and so the use of gasoline yield as one of the objective functions is sufficient. The kinetic model[32] used here is not detailed enough to predict the yield of diesel, and so the latter is not included. In contrast, an increase in the yield of gasoline has an adverse effect on (increase in) the coke formation. This coke decreases the activity of the catalyst, and needs to be burnt off in the regenerator, requiring higher amounts of feed air. Burning of the coke results in the formation of CO and CO_2. The former needs to be converted to CO_2 in the dilute phase before the gases enter the cyclones. This after-burning of CO can produce very high temperatures. There are usually two options available: one is to carry out full combustion in the regenerator, so that the CO emitted in the flue gas is very low. The other is to carry out only partial combustion in the regenerator and allow emission of higher amounts of CO from this unit. The flue gas is then sent to a CO reboiler where it is converted to CO_2 before being emitted finally to the atmosphere. The full combustion mode of the FCCU requires large amounts of air supply. This automatically increases the operating costs. In addition, full combustion leads to much higher amounts of

exothermic heat produced, which could create problems. There is also a need to burn off the maximum amount of the coke in the regenerator so as to keep the catalyst activity in the riser at high levels. Based on the above discussion, we could select three objective functions for the study. The first is to maximize the gasoline yield (profitability), the second is to minimize the CO in the flue gas (pollution limit) and the third is to minimize the air flow rate (operating costs). Consideration of all three objective functions simultaneously at the start of any multi-objective study is difficult to attempt and understand, and so two simplified, two-objective function problems are first studied.

The mathematical representations of the two-objective function optimization problems for the FCCU are:

Problem Nos. 1 and 2:

$\text{Max } I_1(\mathbf{u}) = \text{gasoline yield}$ (a)

$\text{Min } I_2(\mathbf{u}) = F_{air}$ (b)

subject to (s. t.):

$700 \text{ K} \leq T_{rgn} \leq 950 \text{ K}$ (c)

$C_{rgc} \leq 1\%$ (d)

CO in flue gas ≤ 8 % (Problem 1), or

CO in flue gas ≤ 1000 ppm (Problem 2) (e)

where

$\mathbf{u} = \{T_{feed}, T_{air}, F_{cat}, F_{air}\}$ (f) (2)

The following bounds are used for the four decision variables

$575 \leq T_{feed} \leq 670 \text{ K}$ (a)

$$450 \leq T_{air} \leq 525 \text{ K} \quad \text{(b)}$$

$$115 \leq F_{cat} \leq 290 \text{ kg/s} \quad \text{(c)}$$

$$11 \leq F_{air} \leq 46 \text{ kg/s} \quad \text{(d)} \quad (3)$$

The feed preheat temperature, T_{feed}, is selected as a decision variable because it plays a major role in controlling the heat balance in the FCCU. The lower limit of T_{feed} is selected so as to supply sufficient heat required for the cracking and vaporization of the feed. Too low a value of T_{feed} results in a decrease in the riser temperature which, ultimately, decreases the yields of gasoline, LPG, etc. The upper limit[14] of T_{feed} is decided so as to prevent coking of the heating coils in the preheater. The riser top and the regenerator temperatures are functions of the catalyst circulation rate, F_{cat}, and the air flow rate, F_{air}. The lower and upper bounds of the catalyst flow rate, F_{cat}, are taken such that the catalyst-to-feed flow ratio, F_{cat}/F_{feed}, (keeping F_{air}/F_{feed} constant) lies between[14] 4 and 10, respectively. Similarly, the bounds on the air flow rate, F_{air}, are taken such that the air-to-feed flow ratio, F_{air}/F_{feed}, (keeping F_{cat}/F_{feed} constant) lies between[14] 0.4 to 1.6. Below and above these ratios, 'trivial steady states[14] exist, that have no relevance in industrial operations. The lower and upper bounds of the air preheat temperature, T_{air}, are determined by the amount of heat that air can pick up in actual operations. Too low a value of T_{air} results in a cooling of the regenerator, while too high a value has the opposite effect. The first end-point constraint (Eq. 2c) on T_{rgn} is incorporated so as to maintain reasonable temperatures in the dense bed. Too low a value of T_{rgn} decreases the temperature of the regenerated catalyst, which causes a decrease in the riser temperature, which, in turn, leads to a decrease in the yields of gasoline, LPG, etc. Too high a value of T_{rgn} reduces the catalyst activity rapidly and

also causes damage to the catalyst in the regenerator. The second end-point constraint (Eq. 2d) is on the coke on regenerated catalyst. Too high a coke content on the regenerated catalyst results in a decrease in the catalyst activity, which automatically decreases the yields of gasoline, LPG, etc. The third end-point constraint (both possibilities in Eq. 2e) is put on the amount of CO in the flue gas. The two-objective optimization problem is solved in order to get the optimal conditions for operating the FCCU in the partial combustion mode (Problem 1) or the full combustion mode (Problem 2). The value used for CO in Problem 1 is somewhat higher than the industrial value available to us.

It is found (see Results and Discussion later) that the maximum amount of CO allowed in the flue gas (Eq. 2e) plays an important role in determining the optimal conditions for FCCU operation. Too low a limit results in large amounts of heat liberated in the regenerator (due to after-burning). This ultimately results in very large temperature increases in the dilute phase of the regenerator. This could cause damage to the cyclones.

In order to develop further insight, we studied yet another two-objective function optimization problem:

Problem No. 3

$\text{Max } I_1(\mathbf{u}) = \text{gasoline yield}$ (a)

$\text{Min } I_2(\mathbf{u}) = \%\text{ CO in the flue gas}$ (b)

$700\text{ K} \leq T_{rgn} \leq 950\text{ K}$ (c)

$C_{rgc} \leq 1\%$ (d)

where

$$\mathbf{u} = \{T_{feed}, T_{air}, F_{cat}, F_{air}\} \quad \text{(e)} \quad (4)$$

The bounds on the decision variables (Eqs. 3 a-d) are the same as in Problems 1 and 2. The results of this study show that the solutions in the partial-combustion zone (with higher CO levels) are not picked up by NSGA-II since they are inferior to those in the complete-combustion zone (with CO at ppm levels). This is because one of the objective functions is to minimize the CO in the flue gas.

In order to encompass Problems 1-3 into a single interesting multi-objective optimization problem, we solved the following three-objective function optimization problem:

Problem No. 4:

$$\text{Max } I_1(\mathbf{u}) = \text{gasoline yield} \quad \text{(a)}$$

$$\text{Min } I_2(\mathbf{u}) = F_{air} \quad \text{(b)}$$

$$\text{Min } I_3(\mathbf{u}) = \%\ CO \text{ in the flue gas} \quad \text{(c)}$$

s.t.

$$700\ K \leq T_{rgn} \leq 950\ K \quad \text{(d)}$$

$$C_{rgc} \leq 1\% \quad \text{(e)} \quad (5)$$

The bounds on the decision variables (Eqs 3 a-d) are the same as in Problems 1-3.

Most workers in the field have used the penalty-function approach while solving optimization problems with end-point constraints.[54] This works when the process is not too complex. In the case of the FCCU, the model is quite complex and a different approach is being used. Since GA generates solutions randomly, the moment a solution is generated, it is checked to see if it is able to satisfy *all* the end-point constraints. If it

does not, we do not accept it as a member of the population, and generate another chromosome till these conditions are satisfied. This enables all the members in a population to satisfy all the constraints. A similar thing is done when daughter chromosomes are obtained after crossover and mutation. This technique was found to be superior to the conventional penalty function approach[40] (penalty proportional to the deviation) for the present problem. It enables the generation of a wider variety (diversity) of solutions. However, it is a little slow in the beginning.

CHAPTER 3

RESULTS AND DISCUSSION

A computer code was written in MS Fortran Power Station™ to obtain the results of the multi-objective optimization problems. The code was tested (using a single chromosome) for *simulation* of a few runs for which industrial data was available to us, and compared with results obtained by Dave.[32] The parameters describing the FCCU are given in Table 4. The initial guesses of T_{rgn} and C_{rgc} were 900 K and 0.002 kg coke/kg catalyst, respectively. The parameters associated with GA for Problems 1-4 are given in Table 5. The computational time required for solving Problem 1 is 12 hr on a Pentium 4 (1.7 GHz) machine. The results for Problems 1 and 2 are shown in Fig. 3. If we go from any one point to another in Fig. 3 a, we find that one objective function, e.g., gasoline yield, improves (increases) while the other, the air flow rate, worsens (increases). These plots are, therefore, Pareto sets. The decision variables associated with each of these non-dominated solutions are shown in Figs. 3 b, c, and d. Figs. 3 e-q show several important state variables under these conditions.

We first discuss the results for *Problem 1*. It can be observed from Figs. 3 b-d that the air and the feed preheat temperatures for most of the optimal solutions lie at their upper bounds, and that the catalyst flow rate is the most sensitive of the decision variables. A close study of Fig. 3 d shows that the catalyst flow rate first increases to its upper bound (with simultaneous changes in the air and feed preheat temperatures) as the air flow rate increases, and then drops sharply, before increasing again. In this second region, the other two decision variables remain essentially constant at their upper bounds. Some scatter is observed in Fig. 3 b. This is because of the relative insensitivity of the air

TABLE 5
GA Parameters[46] Used in this Study

Parameter	Problems 1, 2, and 4	Problem 3
Total chromosome length (N_{chr})	40	40
Number of generations (N_{ga})	50	90
Population size (N_P)	50	100
Crossover probability (p_c)	0.95	0.95
Mutation probability (p_m)	0.05	0.05

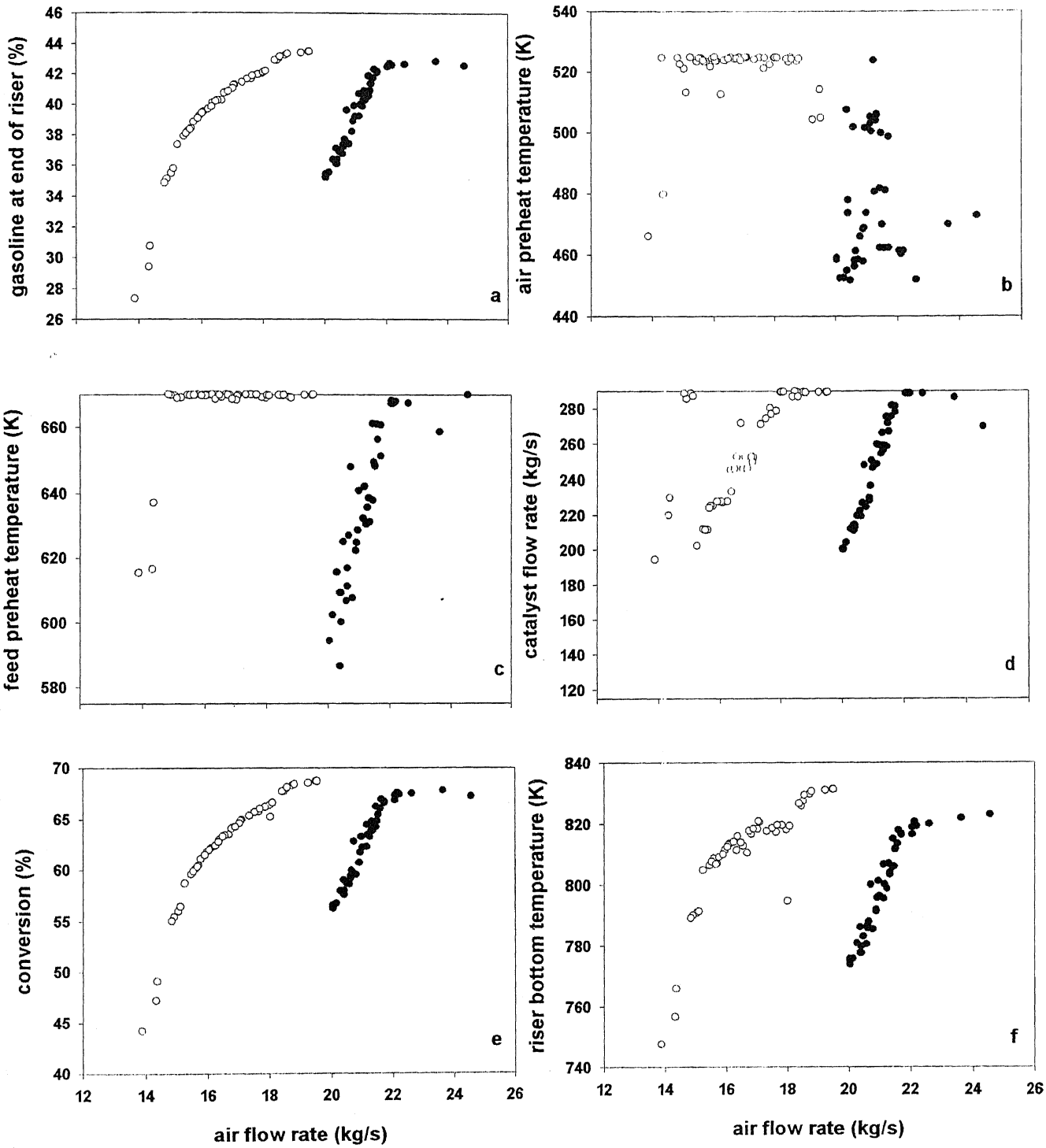

Figure 3 Pareto set, decision variables and state variables of optimal solutions for Problem 1(unfilled circles) and Problem 2 (filled circles)

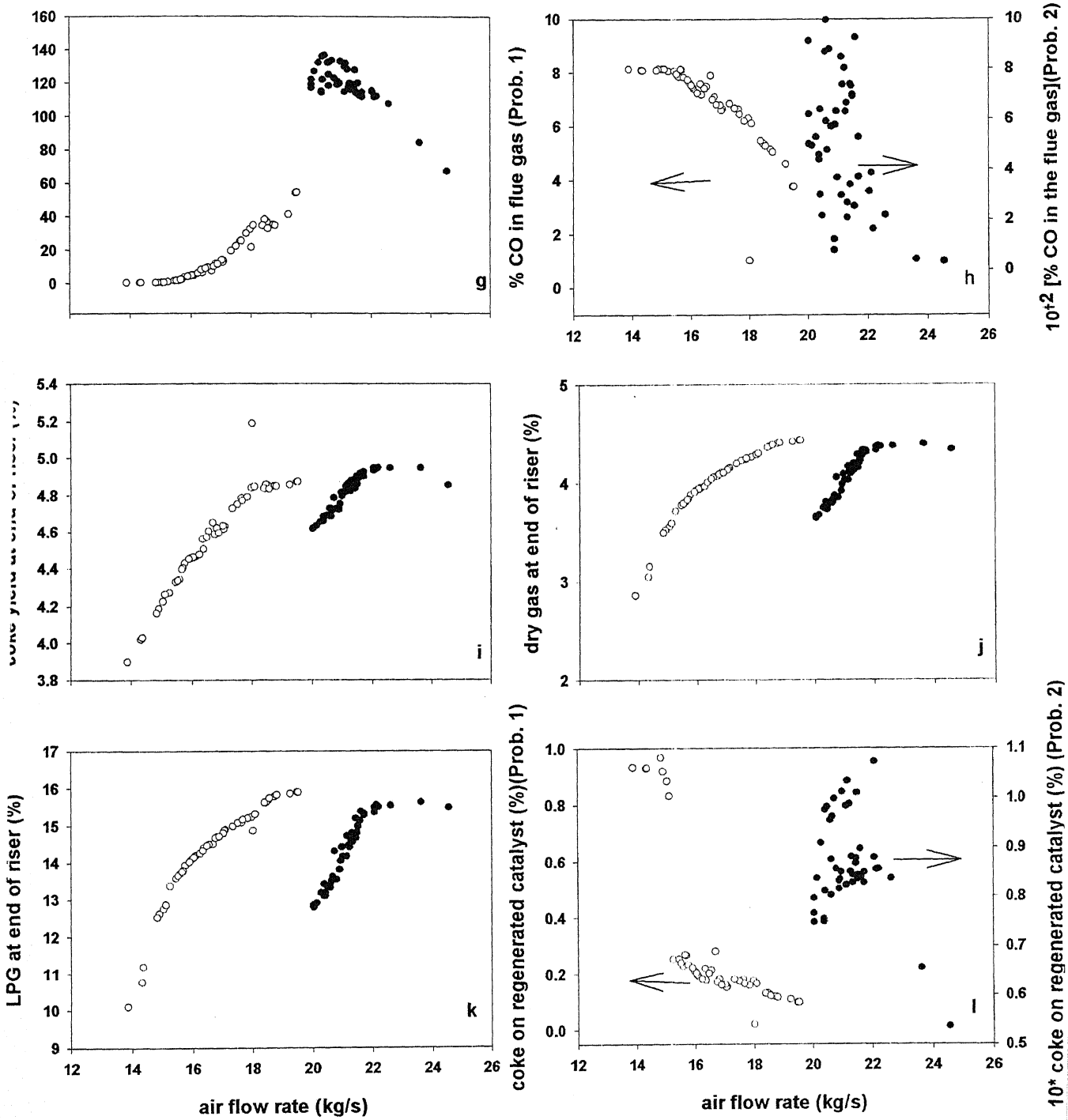

Figure 3 (contd.) Pareto set, decison variables and state variables of optimal solutions for Problem 1(unfilled circles) and Problem 2 (filled circles)

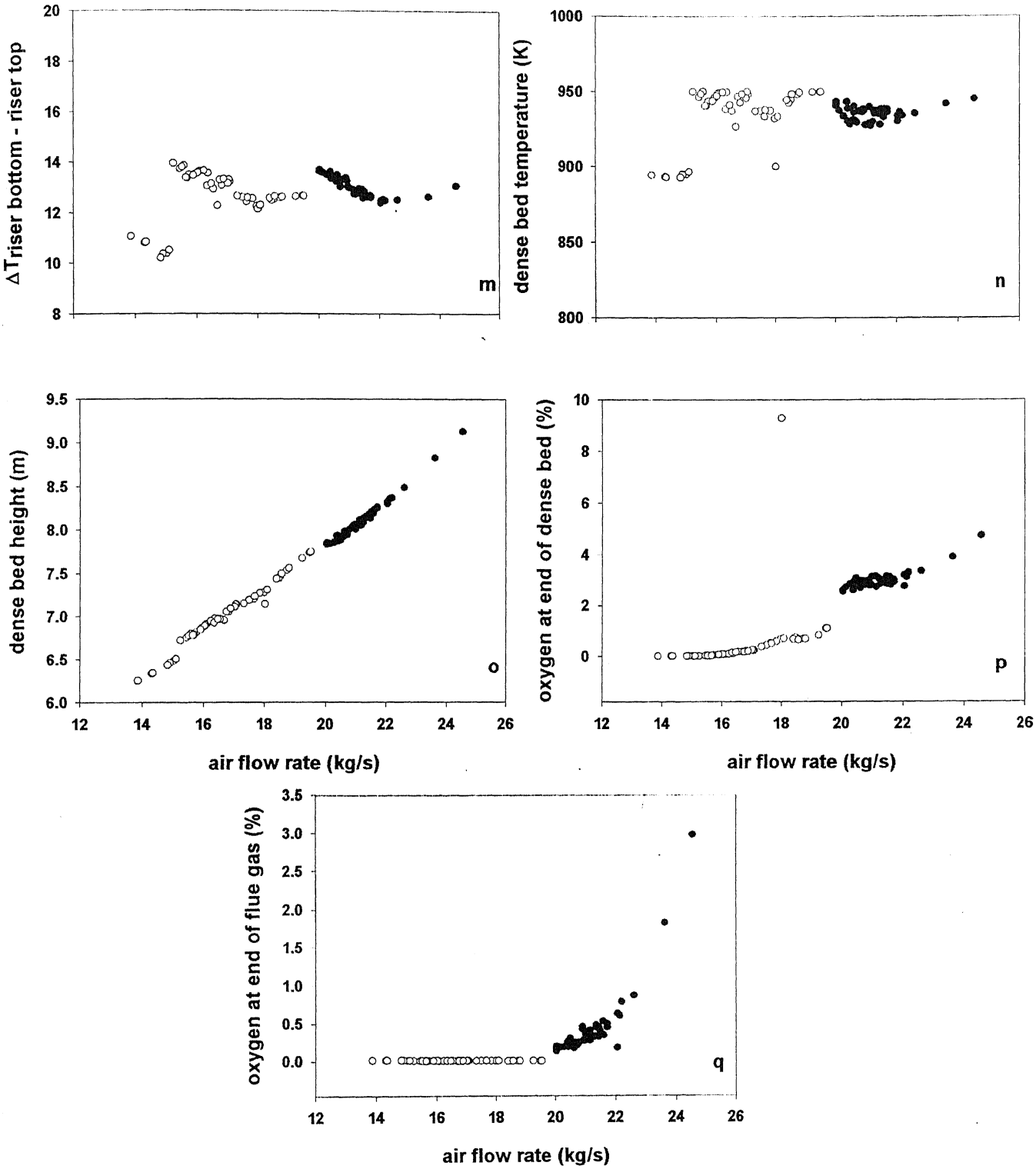

Figure 3 (contd.) Pareto set, decision variables and state variables of optimal solutions for Problem 1 (unfilled circles) and Problem 2 (filled circles)

preheat temperature in influencing the Pareto. Similar insensitivities of decision variables leading to scatter have been observed in our earlier studies,[53] too, and one could, if one wished to, easily select constant values of such variables and solve the multi-objective optimization problem again. Increase in the feed preheat temperature results in an expected increase in the temperature at the base of the riser (Fig. 3 f). An increase in the air preheat temperature, however, increases the heat input to the regenerator which causes a rise in the temperature of the regenerated catalyst (Fig. 3 n) and, ultimately, increases the riser base temperature. Similarly, an increase in the catalyst flow rate results in an increase in the cracking reactions. This leads to an increase in the total conversion (Fig. 3 e) as well as in the individual yields of gasoline, dry gas and LPG (Figs. 3 a, j, k). Simultaneously, this leads to an increase in the amount of coke formed (Fig. 3 i) in the riser. In order to satisfy the constraint on C_{rgc} (Eq. 2 d), the decision variables at lower values of the air flow rate in the Pareto set (Fig. 3 a) take on lower values compared to values at higher air flow rates. Increase in any of the decision variables (except the air flow rate) in this region (lower air flow rates) of the Pareto results in higher coke formation in the riser. Under these conditions, the amount of oxygen available both at the feed-end and at the top of the dense bed (Fig. 3 p) in the regenerator, is low. This results in the coke on the regenerated catalyst (Fig. 3 l) to lie at its maximum permissible value. Also, this reduces the after-burning of CO in the dilute phase of the regenerator, and leads to lower values of the temperature increase (Fig. 3 g) there. In contrast, at higher air flow rates on the Pareto set, more oxygen becomes available at the end of the dense bed (Fig. 3 p). This causes after-burning of CO and raises the temperature in the dilute phase. This also leads to a decrease in the coke on the regenerated catalyst, even though more coke is formed in the riser under these conditions. It is observed from Fig. 3 h that the CO

in the flue gas is at reasonably high levels of around 4 - 8% for all the optimal solutions in Problem 1 (partial-combustion problem).

Problem 2 constraints the CO in the flue gas to lie at low levels (complete-combustion problem). Fig. 3 a shows the Pareto set for this problem too. Clearly, higher air flow rates are necessary to achieve this. The corresponding decision and state variables for these solutions are shown in Figs. 3 b-q. All the parameters (conversion, gasoline yield, coke formed in the riser, dry gas yield, LPG yield, temperature at the base of the riser) show almost similar trends as for Problem 1. However, there is a dramatic increase in the temperature in the dilute phase (Fig. 3 g). This is because the air supplied is quite high compared to values in Problem 1, resulting in the availability of more oxygen at the end of the dense bed (Fig. 3 p) in the regenerator for the after-burning of CO in the dilute phase. The amount of CO in the flue gas now reduces to ppm levels (full-combustion). Also, coke on the regenerated catalyst is at negligible levels under these conditions, since almost all the coke is burnt.

It may be argued that the non-dominating solutions of Problem 2 should form a subset of Problem 1. This is not so. Fig. 3a shows that for the same gasoline yield, Problem 1 leads to lower flow rates. Since the air flow rate is minimized, the algorithm does not pick up the points of Problem 2 while solving Problem 1 (unless it is forced to by the constraint on CO in the flue gas). The computational time required in Problem 2 is extremely high (for 10 generations, it takes over 96 hrs) because the algorithm has to re-generate new chromosomes whenever all the end-point constraints are not satisfied, and in this problem, this happens very frequently.

As mentioned earlier, the solutions in the partial-combustion zone are not picked up by the optimization algorithm in *Problem 3* (refer Appendix IV), since they are inferior to those in the complete-combustion zone (because the CO is being minimized).

With the physical insights (and computational skills to obtain the correct Pareto solutions) now developed, we proceed to solve the more difficult *Problem 4* (Eq. 5) involving three-objective functions. The population size was increased to 100 for this problem, and the number of generations was taken as 90. The computer time was about 48 hr. The code for the three-objective function optimization problem was re-run with two of the objective functions identical (so as to reduce to Problem 1). The results were found to superpose very well with those shown in Fig. 3. This check ensured that the code was (relatively) free of errors. Fig. 4 shows the 3-dimensional plot characterizing the non-dominating Pareto optimal points for Problem 4. This *surface* has been obtained by curve-fitting the several Pareto optimal *points* actually obtained. It is observed that optimal solutions with ppm levels of CO in the flue gas are associated with high air flow rates, and yield larger amounts of gasoline. In contrast, optimal solutions with higher (~7 - 8 %) amounts of CO in the flue gas are associated with lower air flow rates. This is similar to what was observed for Problems 1 and 2. Interestingly, it is found that both the complete-combustion and the partial-combustion zones are obtained in the present problem, simultaneously. It can be observed from Fig. 4 (and detailed tabulated information; not being provided here) that every point on the Pareto surface is equally good (non-dominating) since any point may be worse than another in terms of one or two of the three objectives, but is superior in terms of least one other objective function. If we look at the surface plot closely, we see several maxima and a few adjacent minima. Table 6 shows details of two sets of such maxima-minima combinations. Set I in this

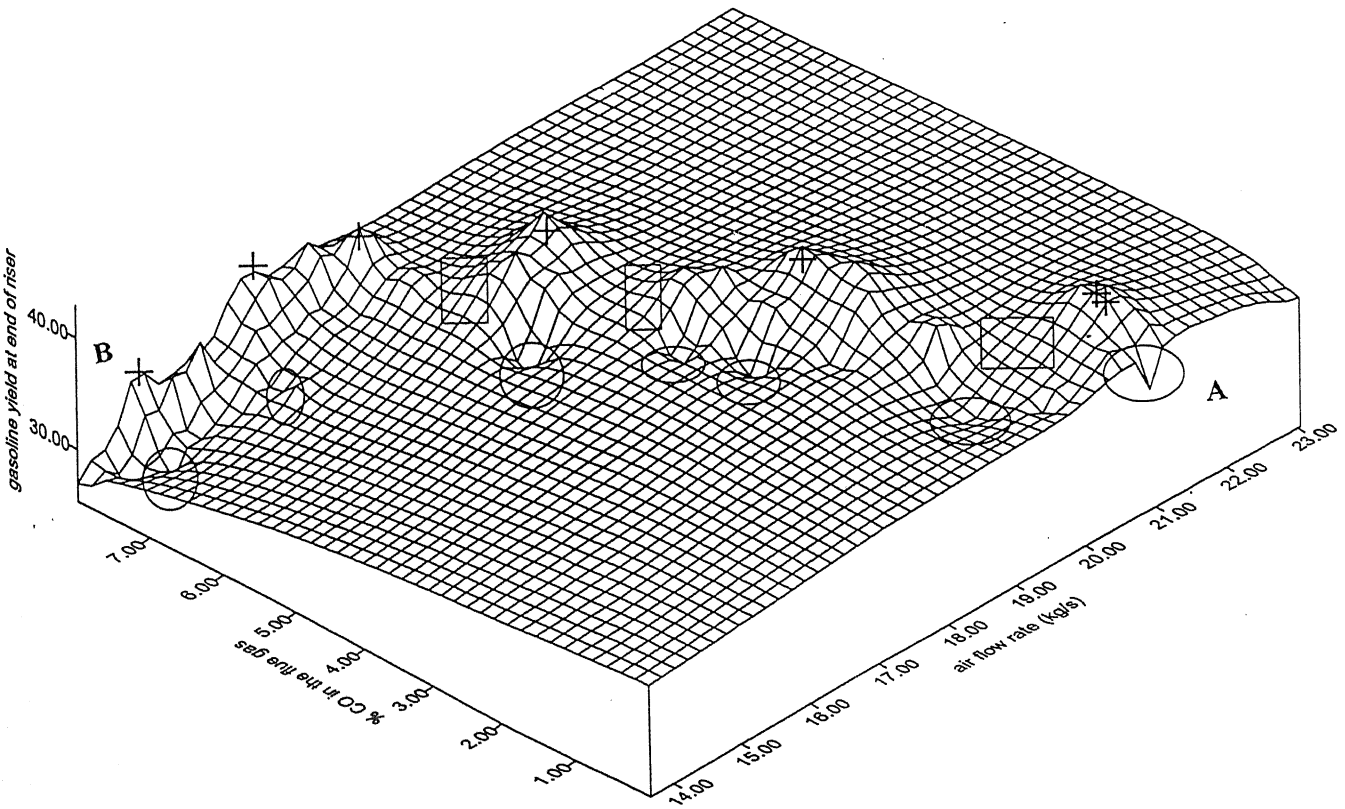

Figure 4 Surface plot for 3-D problem (Problem No. 4)

TABLE 6

Details of Two Sets of Chromosomes in Problem 4

	Set 1		Set 2	
% CO in the flue gas	0.896	0.897	4.268	5.212
Gasoline yield (%)	42.62	35.62	41.49	32.31
Air flow rate (kg/s)	20.92	19.42	18.56	17.33
Air preheat temperature (K)	456.45	471.99	453.01	458.72
Feed preheat temperature (K)	666.75	596.73	665.45	584.84
Catalyst flow rate (kg/s)	285.04	202.93	261.77	192.83

table shows that the air flow rate is lower (better) when the gasoline yield is lower (worse), for almost the same amount of CO in the flue gas, i.e., the peak is superior in terms of the gasoline yield, but the minima is better in terms of the other objective function (air flow rate). A small decrease in the air flow rate (from 20.92 to 19.42 kg/s) is associated with a sharp decrease in the catalyst flow rate (from 285.04 to 202.93 kg/s), which is responsible for the sharp decrease in the gasoline yield (from 42.62 to 35.62 %). Set II in Table 6 shows similar results. This is because of the high sensitivity of the model to the catalyst flow rate in certain regions of the parameter-space. Similar sensitivities were reported by Arbel et al.[14] It is difficult to ascertain, at this stage, if this high sensitivity is real or just a weakness of the model being used here. An improved regenerator model along with the 10- or 12-lump kinetic scheme for the riser will, perhaps, lead to an elimination of such sharp negative peaks in the multiobjective optimization functions.

Some regions of the ridge in-between nearby peaks are shown by rectangles in Fig. 4. There are no optimal *points* in these regions, at least from among the 100 chromosomes obtained in this study. It must also be mentioned here that the computed Pareto solutions occur only in the inner zone in Fig. 4 (where all the maxima and minima lie), and that no solutions exist in the adjacent flat surfaces in Fig. 4 (these are artifacts generated by the graphical package). In other words, in Fig. 4, the Pareto *points* essentially form a series of several hillocks of decreasing heights (with a few nearby minima), starting from the low CO-high air flow end (region A) and curving gently towards the high CO-low air flow end (region B).

If we assign some extra importance to the gasoline yield (a decision-maker's post-Pareto job) than used for generating Fig. 4, the several hills in this plot would

become a *set* of several preferred solutions. The details corresponding to several of the peaks in Fig. 4 (some indicated by +), have been plotted as simpler 2D plots in Fig. 5. The two objective functions (gasoline yield and air flow rate) for these *selected* peaks are shown as a function of the third objective function (% CO in the flue gas) in Figs. 5 a and b, respectively. All the decision variables corresponding to these peaks are plotted in Figs. 5 c-e against percent CO in the flue gas. Several important state variables associated with these points are shown in Figs. 5 f-q. It is observed that for the optimal solutions shown in Figs. 5 a and b, the catalyst flow rate and the feed preheat temperature lie near their upper bounds. This is because high (~ 40 %) values of the gasoline yield require high values of both these variables. The constraint on C_{rgc} is taken care of by the air flow rate. The constraint on T_{rgn} can be satisfied either by adjusting the air flow rate or by adjusting the air preheat temperature. Minimization of the air flow rate leaves T_{air} as the only variable to satisfy the constraint on T_{rgn}. The plot of the air preheat temperature (Fig. 5 c) shows some scatter. The trends of the total conversion, coke, dry gas and LPG yields and the riser bottom temperature (Figs. 5 g, f, h, j and k, respectively) are similar to those shown by the gasoline yield. As the percent CO in the flue gas decreases (moving from the partial-combustion zone to the complete-combustion zone), the air flow rate is found to increase. This leads to an increase in the oxygen available at the end of the dense bed and its subsequent use in the after-burning of CO. This simultaneously results in an increase in the temperature rise in the dilute phase of the regenerator (Fig. 5 i), as well as a decrease in the coke on the regenerated catalyst (Fig. 5 l). Fig. 5 can be used to advantage by a decision-maker to select an appropriate 'preferred solution' (point of operation), based on his or her intuition, something that is often not quantifiable.

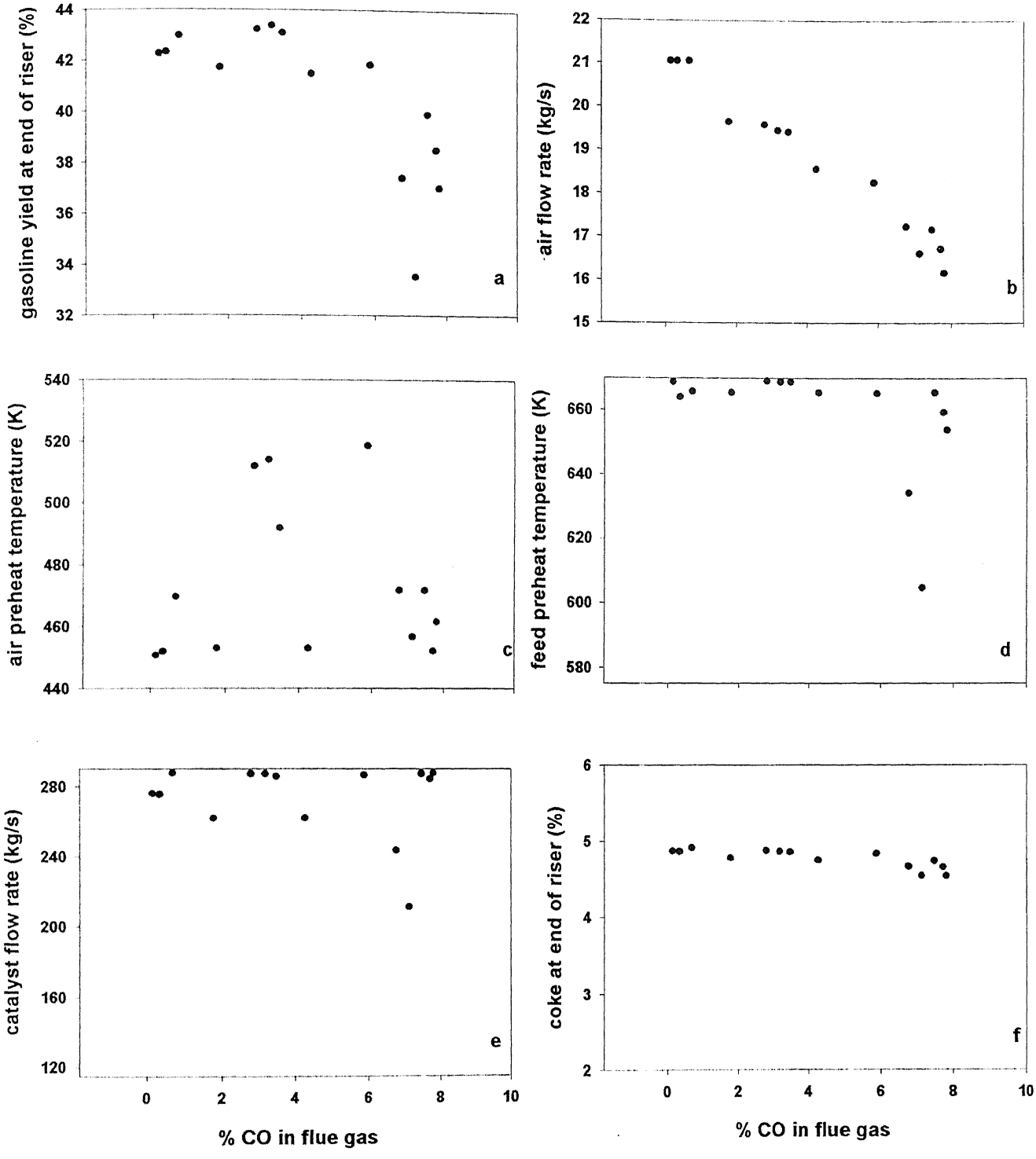

Figure 5 Pareto set, decision variables and state variables for selected optimal solutions (peaks) of Problem 4 (3D problem)

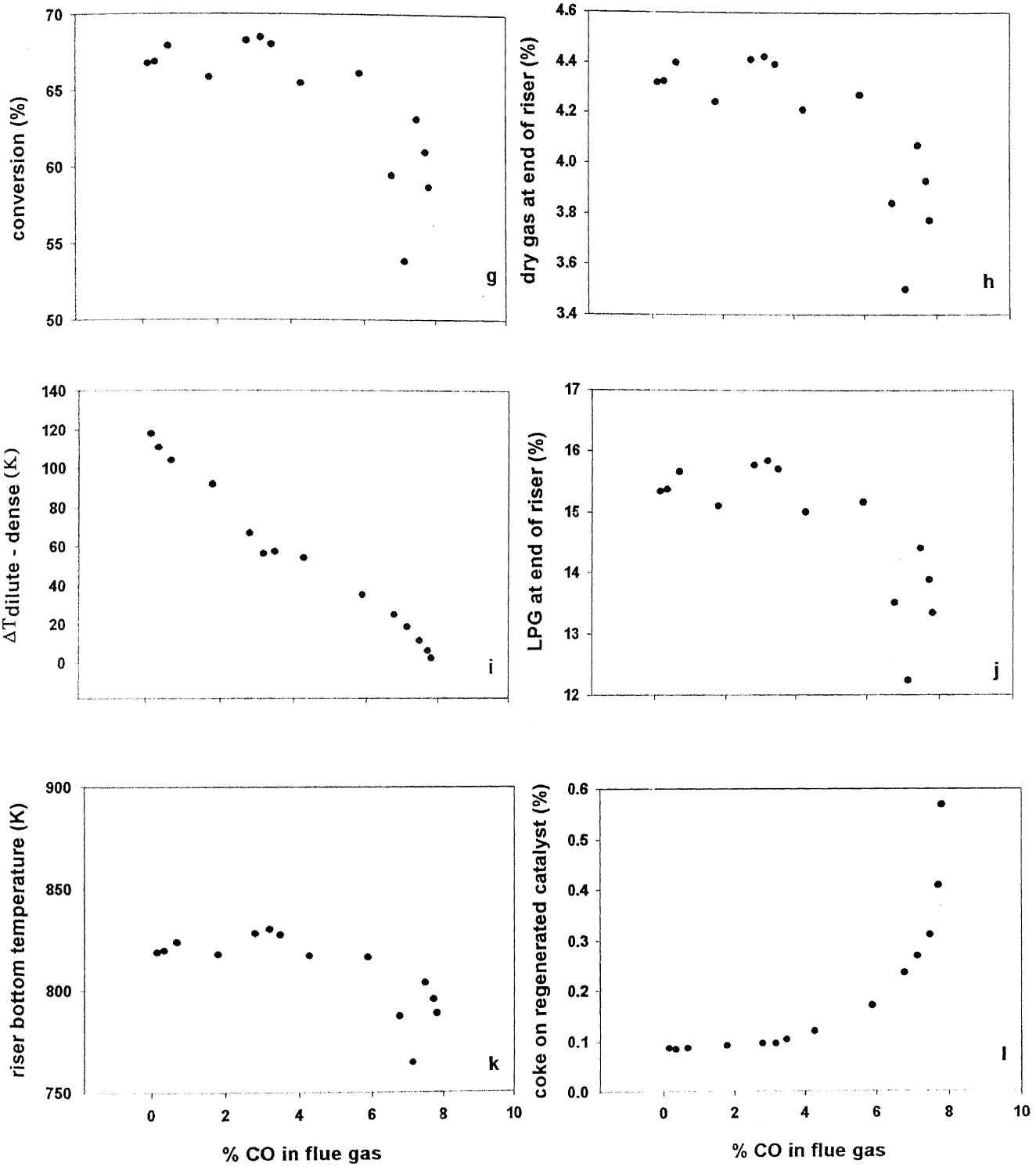

Figure 5 (contd.) Pareto set, decision variables and state variables of selected optimal solutions (peaks) of Problem 4 (3D problem)

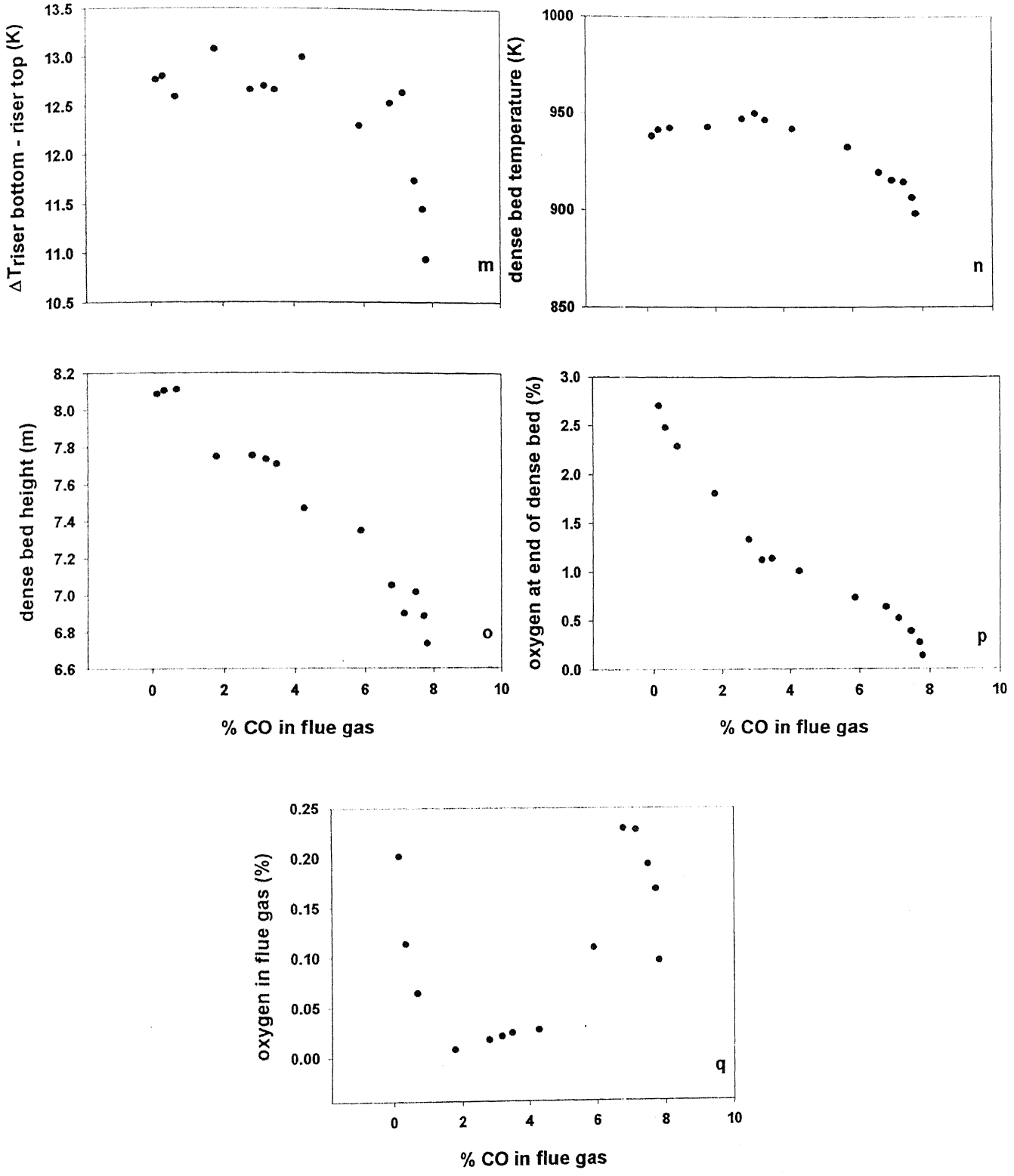

Figure 5 (contd.) Pareto set, decision variables and state variables of selected optimal solutions (peaks) of Problem 4 (3D problem)

Appendix V shows the change in the objective functions over the generations for the Problem 4.

We also studied the effect of varying the computational parameters[46] associated with GA on the 3-D Pareto set (results not shown for the sake of brevity). It is observed that by changing the mutation probability, P_m, from 0.05 to 0.025 (refer Appendix VI), there is hardly any effect on the Pareto-optimal solutions (the Paretos superpose). Similarly, changing the crossover probability, P_c, from 0.95 to 0.975 does not have much effect on the scatter of the optimal Pareto-solutions (reger Appendix VII). In the first five generations (Problem 4), the scatter in the Pareto set reduces as the generations evolve. However, after this relatively small changes occur.

CHAPTER 4

CONCLUSIONS AND RECOMMENDATIONS FOR FUTURE WORK

The present study provides a set of optimal solutions for FCCU operation in an existing industrial refinery. The procedures are quite general and can be applied to any other unit. The optimal results can be broadly classified into two regions, the full-combustion and the partial-combustion modes. In order to study both of these simultaneously one has to solve a three-objective function optimization problem. This study provides a thorough understanding of all aspects of FCCU operating under optimal conditions. Pareto solutions provide an opportunity to an engineer to operate an industrial unit optimally.

Recommendations for Future Work

The present work should further be extended in order to study the multiplicities observed in the 3-D problem in detail. The present off-line optimization study should further be extended to on-line optimization. A more rigorous model should be used for the prediction of all the unaccounted variables in the present study.

REFERENCES

1. Avidan, A. A.; Shinnar, R. Development of Catalytic Cracking Technology. A Lesson in Chemical Reactor Design. *Ind. Eng. Chem. Res.* **1990**, 29, 931.
2. Weekman, V. W., Jr. Kinetics and Dynamics of Catalytic Cracking Selectivity in Fixed Bed Reactors. *Ind. Eng. Chem., Process Des. Dev.* **1969**, 8, 385.
3. John, T. M.; Wojciechowsky, B. W. On Identifying the Primary and Secondary Products of Catalytic Cracking of Neutral Distillates. *J. Catal.* **1975**, 37, 240.
4. Jacob, S. M.; Gross, B.; Voltz, S. E.; Weekman, V. W., Jr. A Lumping and Reaction Scheme for Catalytic Cracking. *AIChE J.* **1976**, 22, 701.
5. Martin, M. P.; Derouin, C.; Turlier, P.; Forissier, M.; Wild, G.; Bernard, J. R. Catalytic Cracking in Riser Reactors: Core Annulus and Elbow Effects. *Chem. Eng. Sci.* **1992**, 47, 2319.
6. Ancheyta, J. J.; Lopez, I. F.; Aguilar, R. E. 5-lump Kinetic Model for Gas Oil Catalytic Cracking. *Appl. Catal. A.* **1999**, 177, 227.
7. Ford, W. D.; Reineman, R. C.; Vasalos, I. A.; Fahrig, R. J. Modeling Catalytic Cracking Regenerators. Presented at the NPRA Annual Meeting, San Antonio, TX, **1976**, Paper AM7629.
8. Errazu, A. F.; de-Lasa, H. I.; Sarti, F. A Fluidized Bed Catalytic Cracking Regenerator Model. Grid Effects. *Can. J. Chem. Eng.* **1979**, 57, 191.
9. Krishna, A. S.; Parkin, E. S. Modeling the Regenerator in Commercial Fluid Catalytic Cracking Units. *Chem. Eng. Prog.* **1985**, 81, 57.
10. Lee, E.; Groves, F. R., Jr. Mathematical Model of the Fluidized Bed Catalytic Cracking Plant. *Trans. Soc. Comput. Simulation* **1985**, 2, 219.

11. Froment, G. F.; Bischoff, K. B. *Chemical Reactor Analysis and Design*; Wiley: NY, 1990.

12. McFarlane, R. C.; Reineman, R. C.; Bartee, J. F.; Georgakis, C. Dynamic Simulator for a Model IV Fluid Catalytic Cracking Unit. *Comput. Chem. Eng.* **1993**, 17, 275.

13. Kumar, S.; Chadha, A.; Gupta, R.; Sharma, R. CATCRAK: A Process Simulator for an Integrated FCC-Regenerator System. *Ind. Eng. Chem. Res.* **1995**, 34, 3737.

14. Arbel, A.; Huang, Z.; Rinard, I. H.; Shinnar, R.; Sapre, A. V. Dynamic and Control of Fluidized Catalytic Crackers. 1. Modeling of the Current Generation of FCC's. *Ind. Eng. Chem. Res.* **1995**, 34, 1228.

15. Han, I.; Chung, C.; Riggs, J. B. Modeling of a Fluidized Catalytic Cracking Process. *Comput. Chem. Eng.* **2000**, 24, 1681.

16. Arandes, J. M.; Azkoiti, M. J.; Bilbao, J.; de Lasa, H. I. Modeling FCC Units under Steady and Unsteady State Conditions. *Can. J. Chem. Eng.* **2000**, 78, 111.

17. Weekman, V. W., Jr. A Model of Catalytic Cracking Conversion in Fixed, Moving, and Fluid Bed Reactors. *Ind. Eng. Chem., Process Des. Dev.* **1968**, 7, 90.

18. Lee, L.; Chen, Y.; Huang, T.; Pan, W. Four-Lump Kinetic Model for Fluid Catalytic Cracking Process. *Can. J. Chem. Eng.* **1989**, 67, 615.

19. Paraskos, J. A.; Shah, Y. T.; McKinney, J. D.; Carr, N. L. A Kinematic Model for Catalytic Cracking in a Transfer Line Reactor. *Ind. Eng. Chem., Process Des. Dev.* **1976**, 15, 165.

20. Shah, Y. T.; Huling, G. T.; Paraskos, J. A.; McKinney, J. D. A Kinematic Model for an Adiabatic Transfer Line Catalytic Cracking Reactor. *Ind. Eng. Chem., Process Des. Dev.* **1977**, 16, 89.

21. Voltz, S. E.; Nace, D. M.; Weekman, V. W., Jr. Application of a Kinetic Model for Catalytic Cracking – Some Correlations of Rate Constants. *Ind. Eng. Chem., Process Des. Dev.* **1971**, 10, 538.

22. Cerqueira, H. S.; Biscaia, E. C., Jr.; Sousa, A. E. F. Mathematical Modeling and Simulation of Catalytic Cracking of Gas Oil in a Fixed Bed: Coke Formation. *Appl. Catal. A.* **1997**, 164, 35.

23. Voorhies, A., Jr. Carbon Formation in Catalytic Cracking. *Ind. Eng. Chem.* **1945**, 37, 318.

24. Nace, D. M.; Voltz, S. E.; Weekman, V. W., Jr. Application of a Kinetic Model for Catalytic Cracking – Effects of Charge Stocks. *Ind. Eng. Chem., Process Des. Dev.* **1971**, 10, 530.

25. John, T. M.; Wojciechowsky, B. W; Pachovsky, R. A. Coke and Deactivation in Catalytic Cracking. *Advances in Chemistry Series* **1974**, 32, 422.

26. Froment, G. F.; Bischoff, K. B. Non-steady State Behavior of Fixed Bed Catalytic Reactors due to Catalyst Fouling. *Chem. Eng. Sci.* **1961**, 16, 189.

27. Beeckman, J.W.; Froment, G.F. Catalyst Deactivation by Site Coverage and Pore Blockage. *Chem. Eng. Sci.* **1980**, 35, 805.

28. De Lasa, H. I; Grace, J. R. The Influence of the Freeboard Region in a Fluidized Bed Catalytic Cracking Regenerator. *AIChE J.* **1979**, 25, 984.

29. De Lasa, H. I.; Errazu A.; Barreiro E.; Solioz, S. Analysis of Fluidized Bed Catalytic Cracking Regenerator Models in an Industrial Scale Unit. *Can. J. Chem. Eng.* **1981**, 59, 549.

30. Kunii, D.; Levenspiel, O. *Fluidization Engineering*, Wiley: NY, 1969.

31. Ellis, R. C.; Li, X.; Riggs, J. B. Modeling and Optimization of a Model IV Fluidized Catalytic Cracking Unit. *AIChE J.* **1998**, 44, 2068.

32. Dave, D. Modeling of a Fluidized Bed Catalytic Cracker Unit; M. Tech. Thesis, Department of Chemical Engineering, I.I.T., Kanpur, India, 2001.

33. Davis, T. A.; Griffin, D. E.; Webb, P. U. Cat Cracker Optimization and Control. *Chem. Engg. Prog.* **1974**, 70, 53.

34. Webb, P. U.; Lutter, B. E.; Hair, R. L. Dynamic Optimization of Fluid Cat Crackers. *Chem. Engg. Prog.* **1978**, 74, 72.

35. Rhemann, H.; Schwarz, G.; Badgwell, T. A.; Darby, M. L.; White, D. C. On-line FCCU Advanced Control and Optimization, *Hydroc. Process.***1989**, 64.

36. McFarlane, R. C.; Bacon, D. W. Adaptive Optimizing Control of Multivariable Constrained Chemical Processes. 1. Theoretical Development. *Ind. Eng. Chem. Res.* **1989**, 28, 1828.

37. Chitnis, U. K.; Corripio, A. B. On-line Optimization of a Model IV Fluid Catalytic Cracking Unit. *ISA Trans.* **1998**, 37, 215.

38. Khandalekar, P. D.; Riggs, J. B. Nonlinear Process Model Based Control and Optimization of a Model IV FCC Unit. *Comput. Chem. Eng.* **1995**, 19, 1153.

39. Nelder, J. A.; Mead, R. A Simplex Method for Function Minimization. *Computer J.* **1964**, 7, 308; **1965**, 8, 27.

40. Beveridge, G. S. G.; Schechter, R. S. Optimization: Theory and Practice; McGraw-Hill: NY, 1970.

41. Ramasubramanian, S.; Luus, R.; Woo, S.S. Optimization of a Fluidized Catalytic Cracking Unit. Presented at 50th Canadian Chemical Engineering Conference, Montreal, Canada, 2000.

42. Luus, R.; Jaakola, T. H. I. Optimization by Direct Search and Schematic Reduction of the Size of Search Region. *AIChE J.* **1973**, 19, 760.

43. Zhao, W.; Chen, D.; Hu, S. Optimizing Operating Conditions Based on ANN and Modified GAs. *Comput. Chem. Eng.* **2000**, 24, 61.

44. Holland, J. H. Adaptation in Natural and Artificial Systems; University of Michigan Press: Ann Arbor, MI, 1975.

45. Goldberg, D. E. Genetic Algorithm in Search, Optimization and Machine Learning; Addison-Wesley: Reading, MA, 1989.

46. Deb, K. Optimization for Engineering Design: Algorithms and Examples; Prentice Hall of India: New Delhi, India, 1995.

47. Srinivas, N.; Deb, K. Multiobjective Optimization Using Nondominated Sorting in Genetic Algorithms. *Evol. Comput.* **1995**, 2, 106.

48. Deb, K.; Agrawal, S.; Pratap, A.; Meyarivan, T. A Fast Elitist Non-dominated Sorting Genetic Algorithm for Multi-objective Optimization: NSGA-II. *Proceedings of the Parallel Problem Solving from Nature VI Conference.* Paris, France. September 2000.

49. Mitra, K.; Deb, K.; Gupta, S. K. Multiobjective Dynamic Optimization of an Industrial Nylon 6 Semibatch Reactor Using Genetic Algorithm. *J. Appl. Polym. Sci.* **1998**, 69, 69.

50. Bhaskar, V.; Gupta, S. K.; Ray, A. K. Multiobjective Optimization of an Industrial Wiped-film PET Reactor. *AIChE J.* **2000**, 46, 1046.

51. Rajesh, J. K.; Gupta, S. K.; Rangaiah, G. P.; Ray, A. K. Multiobjective Optimization of Steam Reformer Performance Using Genetic Algorithm. *Ind. Eng. Chem. Res.* **2000**, 39, 706.

52. Ravi, G.; Gupta, S. K.; Ray, M. B. Multiobjective Optimization of Cyclone Separators. *Ind. Eng. Chem. Res.* **2000**, 39, 4272.

53. Yuen, C. C.; Aatmeeyata; Gupta, S. K.; Ray, A. K. Multiobjective Optimization of Membrane Separation Modules Using Genetic Algorithm. *J. Membrane Sci.* **2000,** 176, 177.

54. Bhaskar, V.; Gupta, S. K.; Ray, A. K. Applications of Multiobjective Optimization in Chemical Engineering. *Reviews Chem. Eng.* **2000**, 16, 1.

55. Deb, K. Multi-objective Optimization using Evolutionary Algorithms; Wiley: Chichester, UK, 2001.

56. Bhaskar, V.; Gupta, S. K; Ray, A. K. Multiobjective Optimization of an Industrial Wiped-Film PET Reactor: Some Further Insights. *Comput. Chem. Eng.* **2001**, 25, 391.

57. Ancheyta, J. J.; Lopez, I. F; Aguilar, R. E.; Moreno, M. J. C. A Strategy for Kinetic Parameter Estimation in the Fluid Catalytic Cracking Process. *Ind. Eng. Chem. Res.* **1997**, 36, 5170.

58. Oliveira, L. L.; Biscaia, E. C., Jr. Catalytic Cracking Kinetic Models. Parameter Estimation and Model Evaluation. *Ind. Eng. Chem. Res.* **1989**, 28, 264.

59. Yingxun, S. Deactivation by Coke in Residuum Catalytic Cracking. Catalyst Deactivation; Bartholomew, C. H. and Butt, J. B. Eds.; Elsevier: Amsterdam, 1991, 327.

60. Gupta, S. K. Numerical Methods for Engineers; Wiley Eastern/New Age Intl.: New Delhi, India, 1995.

Appendix I

MODEL EQUATIONS[32]

REACTOR

$$\frac{dF_j}{dh} = A_{ris} H_{ris} (1-\varepsilon) \rho_c \sum_{i=1}^{9} \alpha_{ij} r_i ; \quad j = 1, 2, \ldots, 5 \tag{A1}$$

$$r_i = k_{o,i} \exp(-\frac{E_i}{RT}) C_1^2 \phi \; ; \quad i = 1 \text{ to } 4 \tag{A2}$$

$$r_i = k_{o,i} \exp(-\frac{E_i}{RT}) C_2 \phi \; ; \quad i = 5 \text{ to } 7 \tag{A3}$$

$$r_i = k_{o,i} \exp(-\frac{E_i}{RT}) C_3 \phi \; ; \quad i = 8, 9 \tag{A4}$$

$$\varepsilon = \frac{F_{feed} / \rho_v}{F_{feed} / \rho_v + F_{rgc} / \rho_c} \tag{A5}$$

$$\rho_v = \frac{P_{ris} MW_g}{RT} \tag{A6}$$

$$MW_g = \sum_{j=1}^{5} x_j MW_j \tag{A7}$$

$$\phi = (1 + 51 C_c)^{2.78} \tag{A8}$$

$$\frac{dT}{dh} = \frac{A_{ris} H_{ris} \rho_c (1-\varepsilon)}{F_{rgc} Cp_c + F_{feed} Cp_{f_v}} \sum_{i=1}^{9} r_i (-\Delta H_i) \tag{A9}$$

$$T\,(h=0) = \frac{\{[F_{rgc} Cp_c (T_{rgn} - 10.0) + F_{feed} Cp_{fl} T_{feed} - \Delta H_{evp} F_{feed}] - 0.019[F_{rgc} Cp_c (T_{rgn} - 10.0) + F_{feed} Cp_{fl} T_{feed} - \Delta H_{evp} F_{feed}]\}}{F_{rgc} Cp_c + F_{feed} Cp_{fv}} \tag{A10}$$

REGENERATOR

Dense Bed

$$\frac{df_{O_2}}{dz} = -A_{rgn}\left(\frac{r_{10}}{2} + r_{11} + \frac{r_{12}}{2}\right) \qquad f_{O_2}(0) = 0.21F_{air} - \frac{1}{2}f_{H_2O} \tag{A11}$$

$$\frac{df_{CO}}{dz} = -A_{rgn}(r_{12} - r_{10}) \qquad f_{CO}(0) = 0 \tag{A12}$$

$$\frac{df_{CO_2}}{dz} = A_{rgn}(r_{11} + r_{12}) \qquad f_{CO_2}(0) = 0 \tag{A13}$$

$$r_{10} = (1-\varepsilon)\rho_c k_{10}\frac{C_{rgc}}{MW_c}\frac{f_{O_2}}{f_{tot}}P_{rgn} \tag{A14}$$

$$r_{11} = (1-\varepsilon)\rho_c k_{11}\frac{C_{rgc}}{MW_c}\frac{f_{O_2}}{f_{tot}}P_{rgn} \tag{A15}$$

$$r_{12} = \left(x_{pt}(1-\varepsilon)\rho_c k_{12c} + \varepsilon k_{12h}\right)\frac{f_{O_2}f_{CO}}{f_{tot}^2}P_{rgn}^2 \tag{A16}$$

$$f_{H_2O} = F_{rgc}(C_{sc} - C_{rgc})\frac{C_H}{MW_{H_2}} \tag{A17}$$

$$f_{N_2} = 0.79F_{air} \tag{A18}$$

$$\frac{dT_{rgn}}{dz} = 0 \tag{A19}$$

$$T_{rgn}(z=0) = T_{base} + \frac{\begin{aligned}&\{[f_{CO}(Z_{bed})H_{CO} + f_{CO_2}(Z_{bed})H_{CO_2} + f_{H_2O}H_{H_2O} + F_{air}Cp_{air}(T_{air} - T_{base})\\&+ F_{sc}Cp_c(T_{sc} - T_{base})] - 0.11[f_{CO}(Z_{bed})H_{CO} + f_{CO_2}(Z_{bed})H_{CO_2} + f_{H_2O}H_{H_2O} +\\&F_{air}Cp_{air}(T_{air} - T_{base}) + F_{sc}Cp_c(T_{sc} - T_{base})]\}\end{aligned}}{\begin{aligned}&\{[F_{rgc}Cp_c + f_{CO_2}(Z_{bed})Cp_{CO_2} + f_{CO}(Z_{bed})Cp_{CO} + f_{O_2}(Z_{bed})Cp_{O_2} + f_{H_2O}Cp_{H_2O}\\&+ f_{N_2}Cp_{N_2}]\}\end{aligned}}$$

{with $f_i(Z_{bed})$ being the value of f_i at $z = Z_{bed}$} (A20)

$$\varepsilon = \frac{0.305u_1 + 1}{0.305u_1 + 2} \tag{A21}$$

$$u_1 = \frac{F_{air}}{0.3048\rho_g A_{rgn}} \tag{A22}$$

$$\rho_g = \frac{P_{rgn}}{RT_{rgn}} \tag{A23}$$

$$Z_{bed} = 0.3048\ (TDH) \tag{A24}$$

$$TDH = TDH_{20} + 0.1\ (D - 20) \tag{A25}$$

$$\log_{10}(TDH_{20}) = \log_{10}(20.5) + 0.07\ (u_1 - 3) \tag{A26}$$

$$C_{rgc} = [F_{sc}C_{sc}(1-C_H) - \{f_{CO}(Z_{bed}) + f_{CO_2}(Z_{bed}\})MW_c]/[F_{rgc}(1-C_H)];$$

{with $f_i(Z_{bed})$ being the value of f_i at $z = Z_{bed}$} (A27)

Dilute Phase

$$\frac{df_{O_2}}{dz} = -A_{rgn}\left(\frac{r_{10}}{2} + r_{11} + \frac{r_{12}}{2}\right);\ f_{O_2}(0) \text{ same as at the end of dense bed} \tag{A28}$$

$$\frac{df_{CO}}{dz} = -A_{rgn}(r_{12} - r_{10});\ f_{CO}(0) \text{ same as at the end of dense bed} \tag{A29}$$

$$\frac{df_{CC_2}}{dz} = A_{rgn}(r_{11} + r_{12});\ f_{CO_2}(0) \text{ same as at the end of dense bed} \tag{A30}$$

$$\frac{df_C}{dz} = -A_{rgn}(r_{10} + r_{11});\ \text{initial condition from Eq. (A40)} \tag{A31}$$

(r_i as in Eqs. A14 – A16, but with appropriate parameters/variables)

$$\frac{dT_{dil}}{dz} = \frac{A_{rgn}}{Cp_{tot}f_{tot}}\left[H_{CO}(r_{10} - r_{12}) + H_{CO_2}(r_{11} + r_{12})\right] \tag{A32}$$

$$Cp_{tot} = \left(\frac{Cp_{N_2}f_{N_2} + Cp_{O_2}f_{O_2} + Cp_{CO}f_{CO} + Cp_{CO_2}f_{CO_2} + Cp_{H_2O}f_{H_2O} + Cp_C F_{ent}}{f_{tot}}\right) \tag{A33}$$

$$F_{ent} = 0.4535\ WA \tag{A34}$$

$$W = \rho_f Y u_1 \tag{A35}$$

$$\log_{10} Y = \log_{10} 60 + 0.69 \log_{10} X - 0.445 (\log_{10} X)^2 \tag{A36}$$

$$X = \frac{u_1^2}{g D_p \rho_p^2} \quad \text{(see Eq. A22)} \tag{A37}$$

$$\varepsilon_{dil} = 1 - \frac{\rho_{dil}}{\rho_c} \tag{A38}$$

$$\rho_{dil} = \frac{F_{ent}}{0.3048 A_{rgn} u_1} \tag{A39}$$

$$f_C(0) = F_{ent} C_{rgc} \frac{(1 - C_H)}{12} \tag{A40}$$

$$Z_{dil} = Z_{rgn} - Z_{bed} \tag{A41}$$

Appendix II

Elitist Non-dominated Sorting Genetic Algorithm (NSGA-II)

- Main criticisms of NSGA:
  - Computational complexity of sorting
  - Specifying sharing parameters
  - Lack of Elitism (best parents may get lost)
- Total complexity of NSGA-II: M(N**2)
- Total complexity of NSGA: M(N**3)

  M: number of objectives

  N: population size

1. A fast non-dominated sorting approach in NSGA-II:

   In order to sort a population of size N depending upon the principle of non-domination, each chromosome is compared with all the other chromosomes to find if it is dominated.

   Non-domination criteria:

   A chromosome is better than any other chromosome if at least any one of its fitness values is better than the corresponding fitness value of the other chromosome and no fitness value of the first chromosome is worse than any of the corresponding fitness value of the second chromosome.

   This approach in NSGA-II is similar to that of NSGA. Only difference is a better book keeping strategy is used to make the algorithm faster. In this approach, every chromosome is compared with partially filled population for non-domination in

contrast to what we have in NSGA where it is compared with all the other chromosomes. We temporarily put one chromosome (p) in a separate box, and then we add one chromosome (q) from the population to that box, and compare q with all members in the box for non-domination. If any member in the box is dominating q, q is removed. If q dominates any member in the box, that member is removed. But if q is non-dominating to all members in the box, then q is put in the same box and continues with the other members. This is how the temporary box grows with non-dominated chromosomes. When all chromosomes are checked, the chromosomes left in box are assigned with rank, I_{RANK} (Here Front 1 is created so rank assigned is also 1). All the other members (not present in Front 1) are used for evaluating other non-dominated fronts and assigned subsequent ranks.

2. Density Estimation:

One of the criteria for judging the betterment of any evolutionary algorithm is how much diversity it can preserve among its solutions. The original NSGA used the famous sharing function approach for preserving diversity among its population. Major difficulties with sharing approach are its performance depends upon the σ_{share} value and the overall complexity of this approach is quite higher. In NSGA-II, the sharing function approach is replaced with a crowded comparison approach in order to overcome all the above-mentioned difficulties.

The density of each chromosome is estimated by calculating crowding distance. In this, all the chromosomes belonging to a particular front (or all those having the same rank) are sorted according to each objective function value in their ascending order of magnitude. Boundary solutions are assigned with an infinite

distance value (practically speaking a very large value). The intermediate solutions are assigned with a distance value equal to the absolute difference in the function values of two adjacent solutions. This is done with all the other objective functions. The overall crowding distance (I_{DIST}) is calculated as the sum of individual distance values corresponding to each objective. This method is continued for all the other fronts.

3. Initially (at generation = 0) all the parent solutions are sorted based on the non-domination. Each solution is given a rank based on its non-domination level. All these solutions undergo binary tournament selection (Binary tournament selection is carried out using crowded comparison operator, see stage 7), crossover and mutation operations and produce child population, which is equal in size to that of parent size.
4. In NSGA-II, parent solutions and child solutions are mixed together to ensure elitism. Elitism is a concept that helps in preserving the elite members of the population throughout all the generations. By mixing parents and children, elitism is ensured.
5. Once the elitism is done, the whole population (now of size 2N) is sorted on the basis of non-domination approach as explained in stage 1. Solutions belonging to the first non-dominated front (or rank) are the best solutions and should be preserved. Crowding distance is calculated for all the solutions belonging to different ranks as explained in stage 2.
6. Now, if the number of solutions belonging to first non-dominated front (rank 1) is smaller than the total population size (N), all the solutions are included in the new population. The remaining members for the new population are selected from subsequent non-dominated fronts in order of their ranking. This is continued till we

fill up the new population with the members equal to the original population size (N). To ensure exactly N members in the new population, the last front is sorted on the basis of crowded comparison operator as explained in stage 7.

7. Crowded comparison operator:

This is used to compare the two solutions at any stage in the algorithm. We know that every solution has non-domination rank and crowding distance associated with it. The operator is defined as:

If we have two solutions with different ranks, we select the solution with the lower rank (means the one from the better non-domination front)

If we have two solutions belonging to same non-domination front, we select the one, which is located in a lower crowded region.

It can be seen from the algorithm that the sorting is done with a better and faster approach as compared to original NSGA. The diversity is preserved using the crowded comparison operator instead of using the sharing approach as used in NSGA. There is no need to specify any sharing parameter. Even though the crowding distance is calculated in the objective function space, it can also be calculated using the parameter space.

Flowchart:

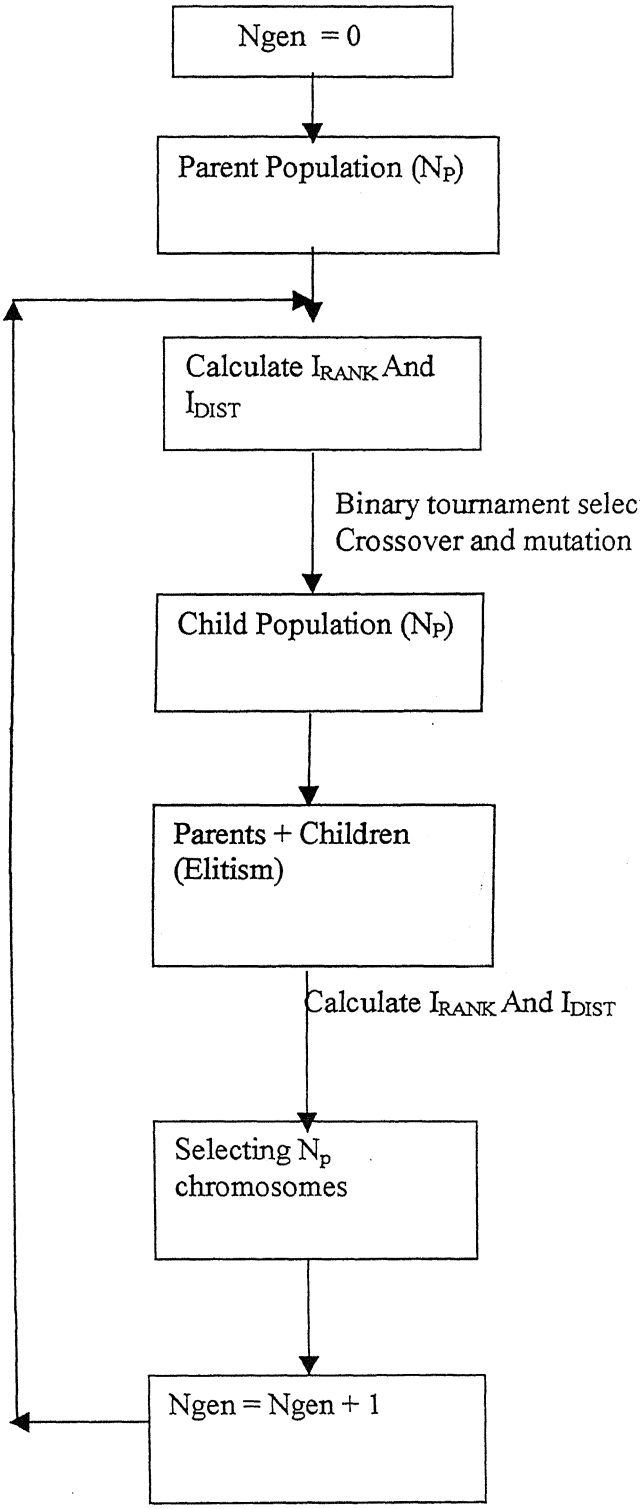
Ngen = 0
Parent Population (N_P)
Calculate I_{RANK} And I_{DIST}
Binary tournament selection, Crossover and mutation
Child Population (N_P)
Parents + Children (Elitism)
Calculate I_{RANK} And I_{DIST}
Selecting N_p chromosomes
Ngen = Ngen + 1

Appendix III

Comparison of Model Results with Industrial Data

	Data Set 1		Data Set 2	
	Data obtained from Industry	Results obtained After tuning	Data obtained from Industry	Results obtained After tuning
Feed flow rate (kg/s)	28.33	28.33	29.08	29.08
Catalyst flow rate (kg/s)	208.33	208.33	205.00	205.00
Feed preheat temp (K)	617.4	617.4	620.7	620.7
Riser pressure (atm)	2.457	2.457	2.506	2.506
Air flow rate (kmol/s)	0.559	0.559	0.5711	0.5711
Air preheat temp(K)	490.3	490.3	493.3	493.3
Regenerator pressure (atm)	2.588	2.588	2.638	2.638
Riser top temperature (K)	765.5	763.0	766.6	767.27
Regenerator temp(K)	930.2	925.0	934.6	935.79
Flue gas temp(K)	945.4	945.34	946.8	953.38
Flue gas oxygen(%)	0.00029	1.21e-1	0.0002	5e-2
Dry gas %	3.1	3.6	3.8	3.635
LPG %	12.1	12.66	12.6	12.821
Gasoline%	32.6	34.92	35.2	35.454
Gas oil %	48.1	44.287	44.1	43.594
Coke %	4.1	4.519	4.3	4.4932

	Data Set 3		Data Set 4	
	Data obtained from Industry	Results obtained After tuning	Data obtained from Industry	Results obtained After tuning
Feed flow rate (kg/s)	29.08	29.08	29.11	29.11
Catalyst flow rate (kg/s)	208.33	208.33	208.33	208.33
Feed preheat temp (K)	621.4	621.4	625.1	625.1
Riser pressure (atm)	2.545	2.545	2.546	2.546
Air flow rate (kmol/s)	0.5759	0.5759	0.5707	0.5707
Air preheat temp(K)	494.4	494.4	493.9	493.9
Regenerator pressure (atm)	2.678	2.678	2.68	2.68
Riser top temperature (K)	768.5	769.83	768.8	770.139
Regenerator temp(K)	937.5	937.37	937.5	936.88
Flue gas temp(K)	949.1	952.0	948.2	948.4
Flue gas oxygen(%)	0.00028	3.92e-2	0.00031	3.45e-2
Dry gas %	3.8	3.7	3.4	3.69
LPG %	12.6	13.0	12.4	13.05
Gasoline%	35.2	36.1477	34.0	36.13
Gas oil %	44.1	42.545	45.6	42.594
Coke %	4.3	4.543	4.6	4.522

Appendix IV

Pareto set, decision variables and state variables for optimal solutions of Problem 3
population size 50; number of generations 50; mutation probability 0.05; crossover probability 0.95

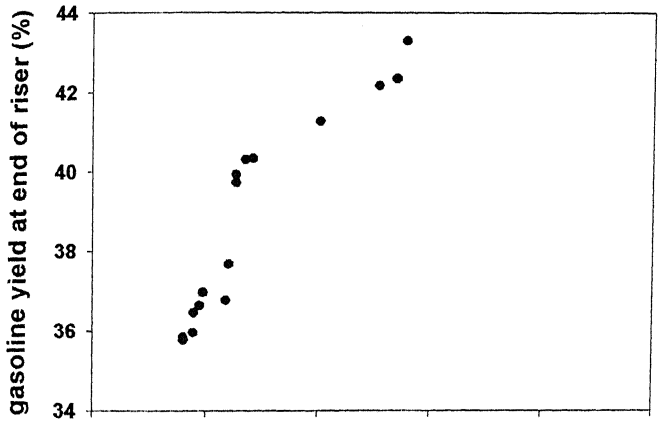

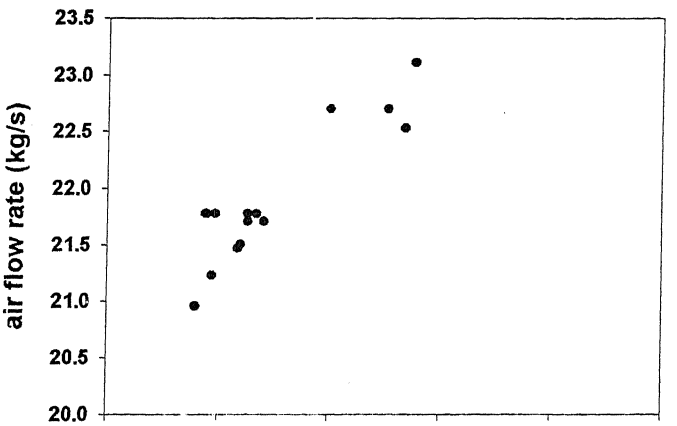

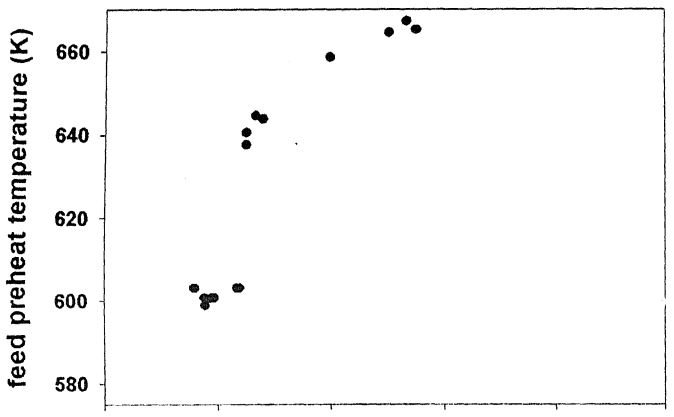

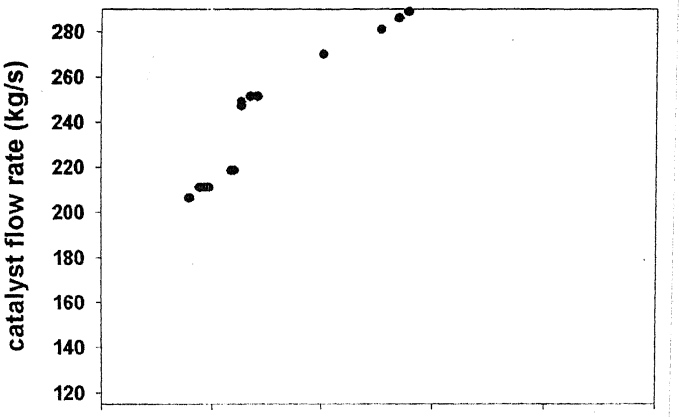

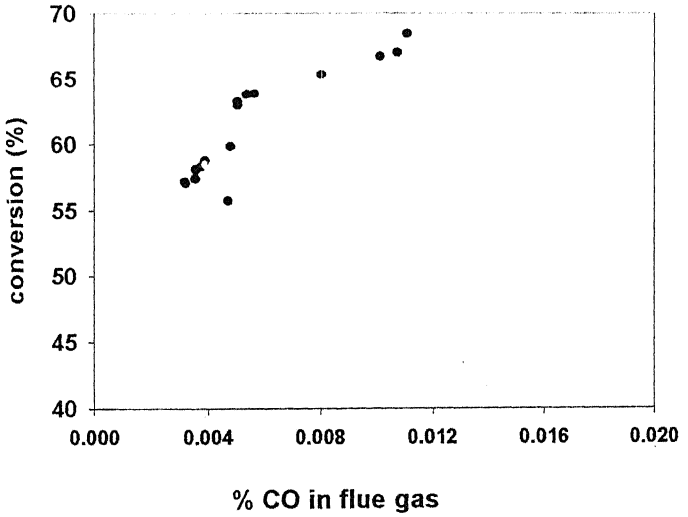

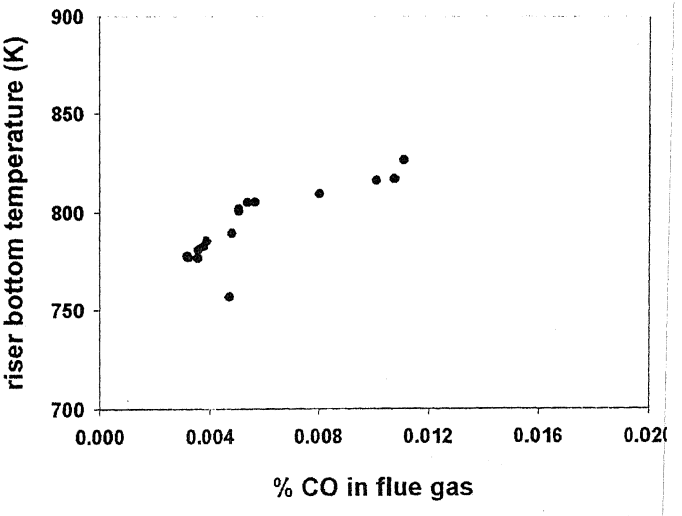

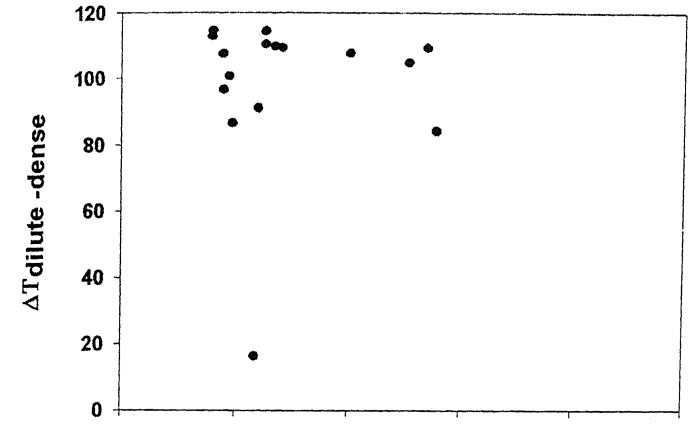
ΔTdilute -dense
120
100
80
60
40
20
0

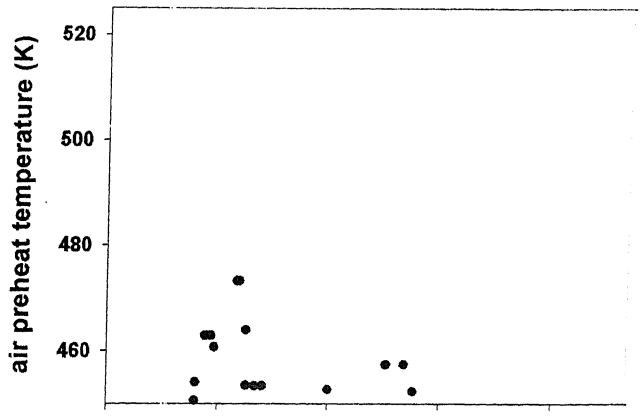
air preheat temperature (K)
520
500
480
460

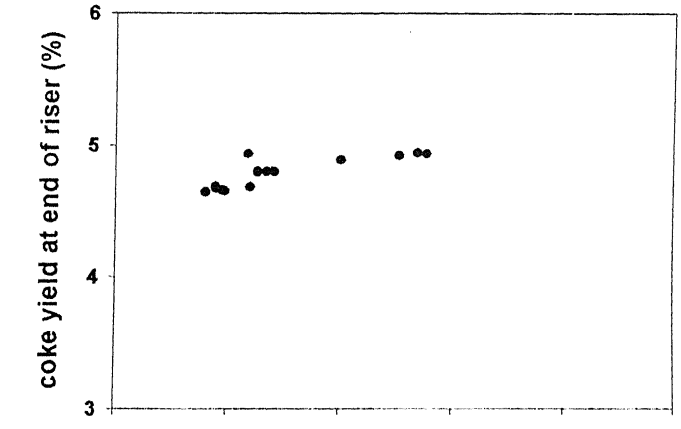
coke yield at end of riser (%)
6
5
4
3

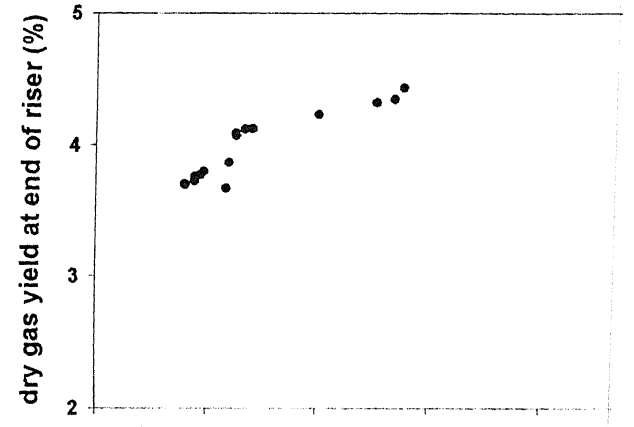
dry gas yield at end of riser (%)
5
4
3
2

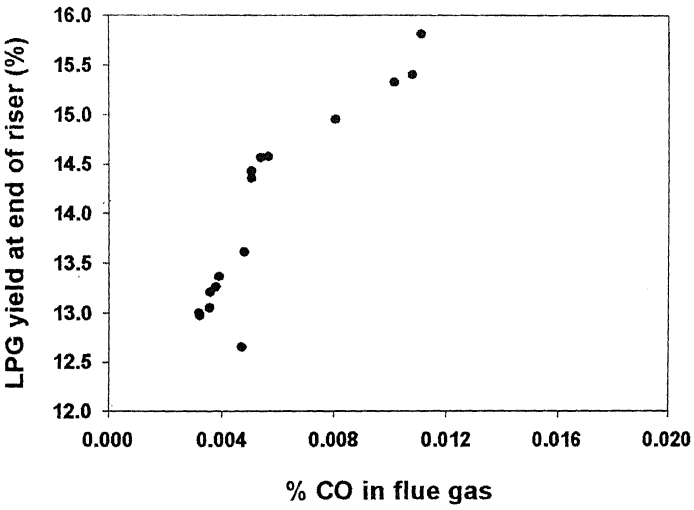
LPG yield at end of riser (%)
16.0
15.5
15.0
14.5
14.0
13.5
13.0
12.5
12.0
0.000
0.004
0.008
0.012
0.016
0.020
% CO in flue gas

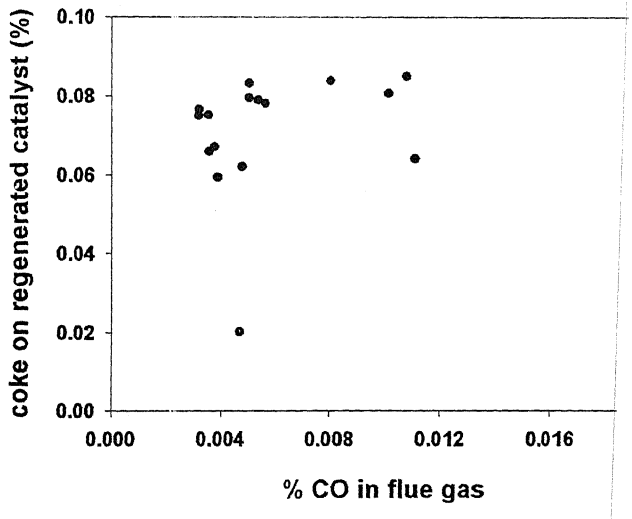
coke on regenerated catalyst (%)
0.10
0.08
0.06
0.04
0.02
0.00
0.000
0.004
0.008
0.012
0.016
% CO in flue gas

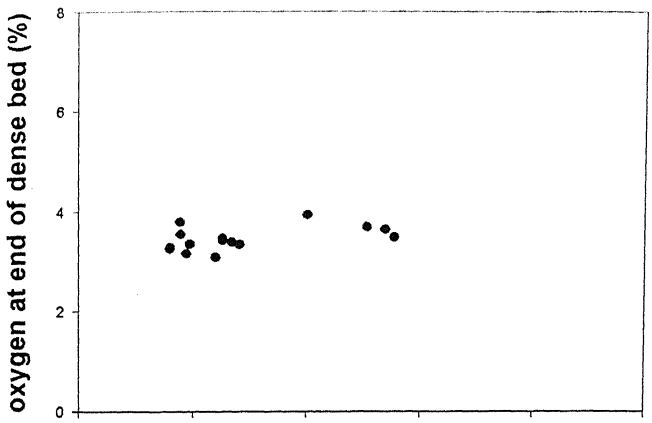
oxygen at end of dense bed (%)
0
2
4
6
8

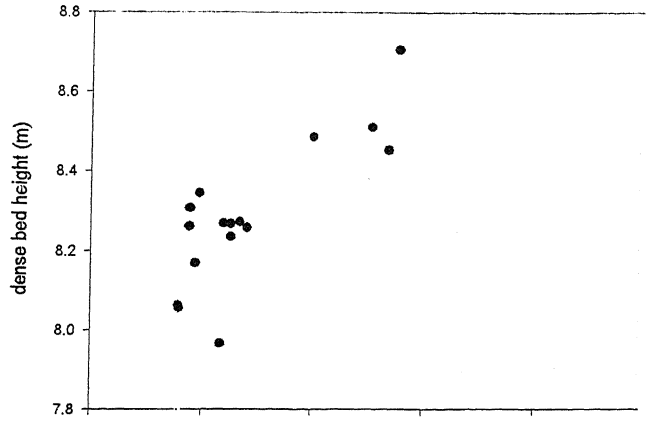
dense bed height (m)
7.8
8.0
8.2
8.4
8.6
8.8

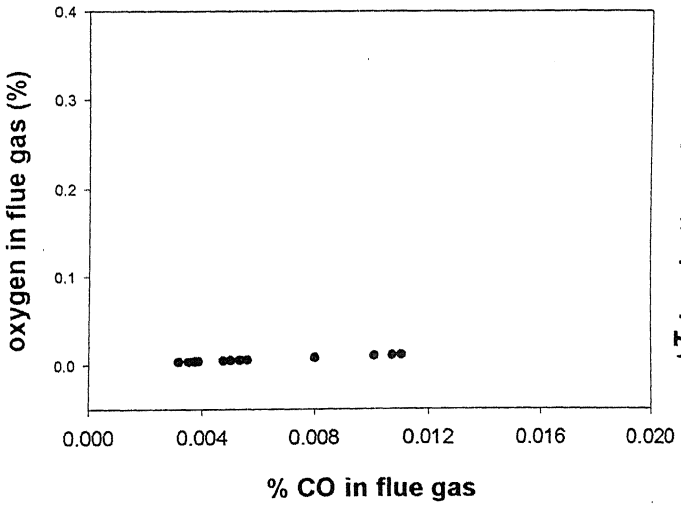
oxygen in flue gas (%)
0.0
0.1
0.2
0.3
0.4
0.000
0.004
0.008
0.012
0.016
0.020
% CO in flue gas

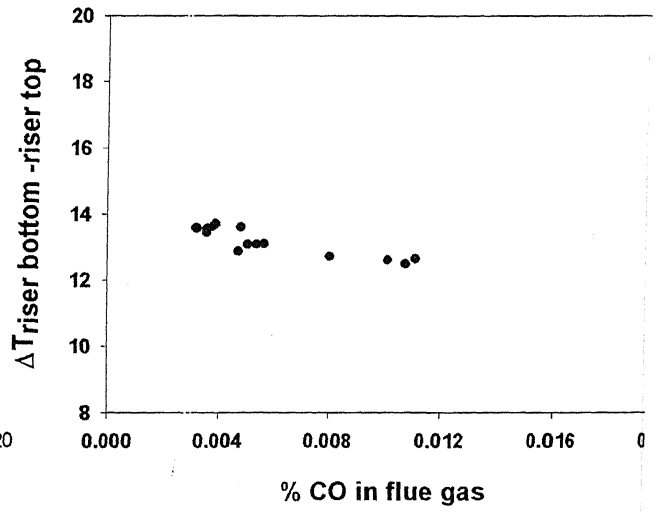
ΔTriser bottom -riser top
8
10
12
14
16
18
20
0.000
0.004
0.008
0.012
0.016
% CO in flue gas

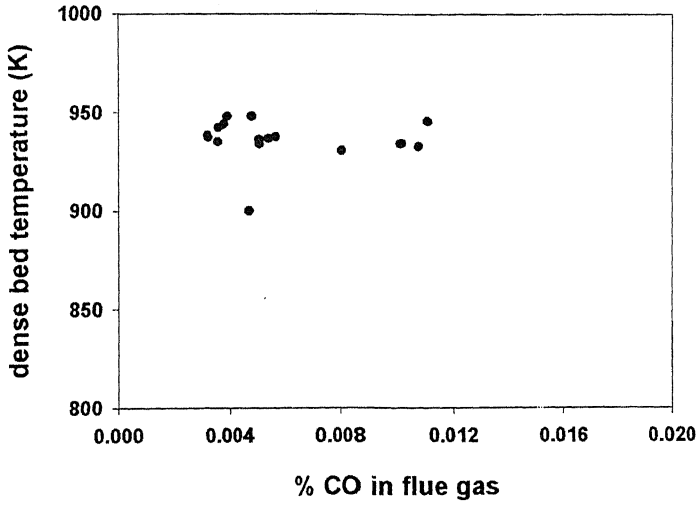
dense bed temperature (K)
800
850
900
950
1000
0.000
0.004
0.008
0.012
0.016
0.020
% CO in flue gas

Appendix V

Evolution of Pareto (Problem 4) over generations

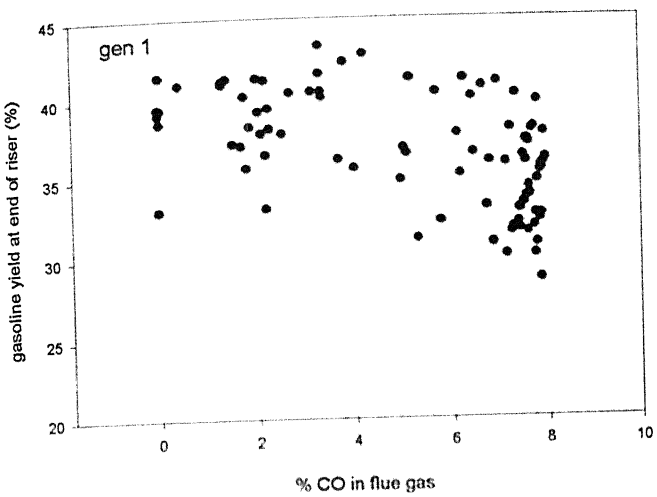

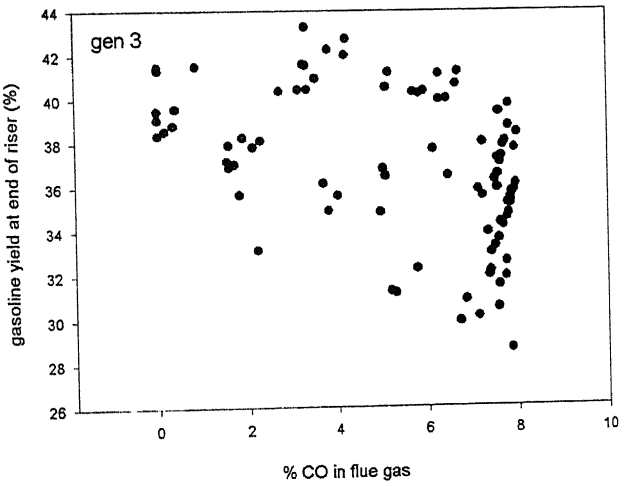

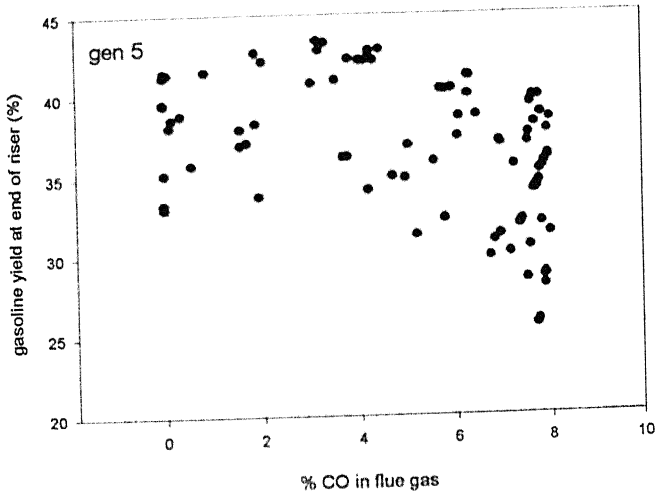

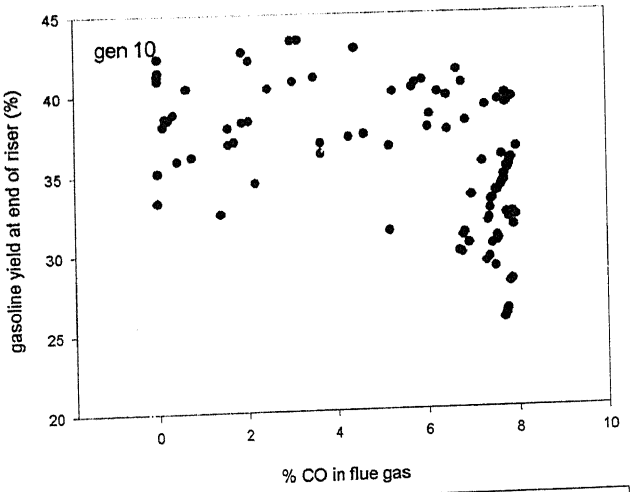

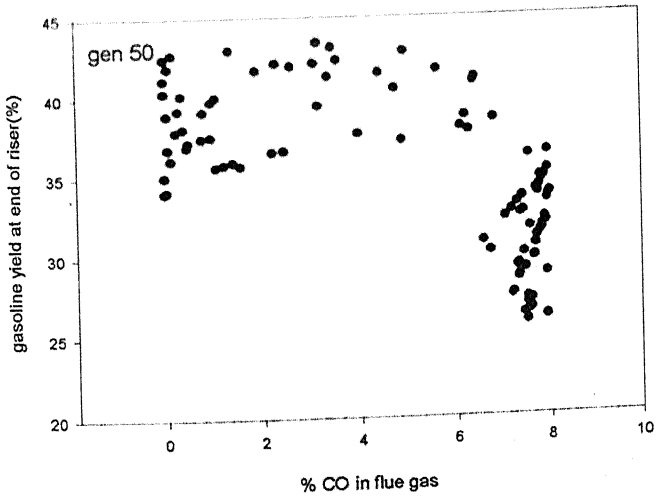

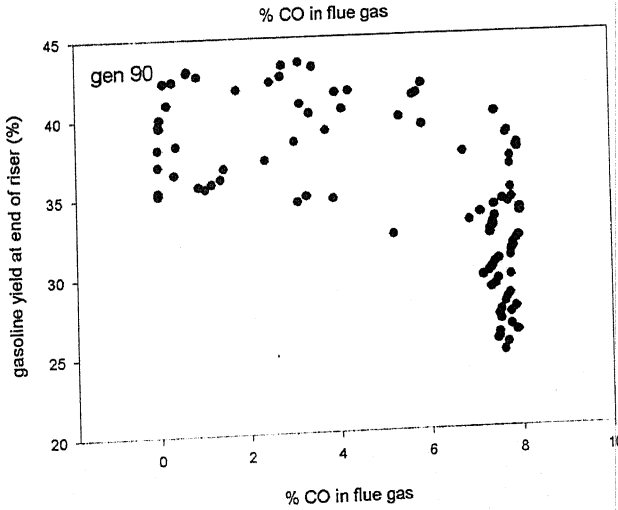

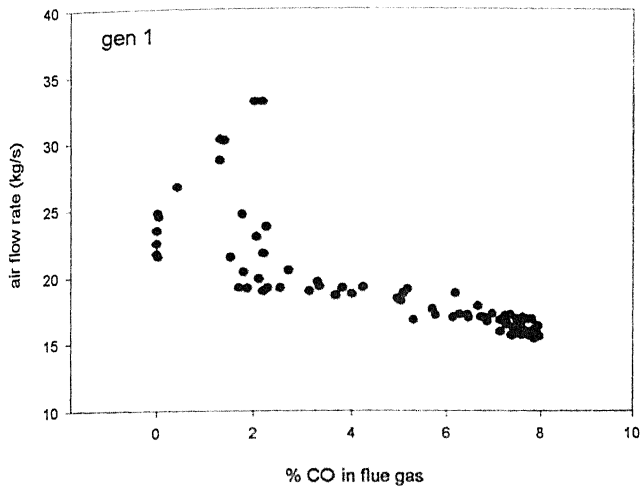
gen 1
air flow rate (kg/s)
% CO in flue gas

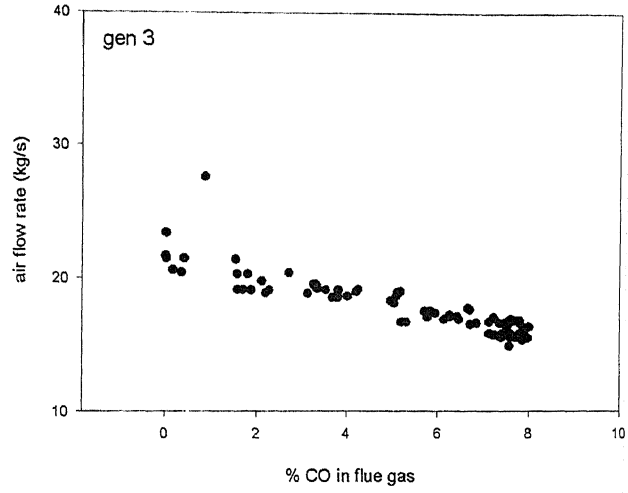
gen 3
air flow rate (kg/s)
% CO in flue gas

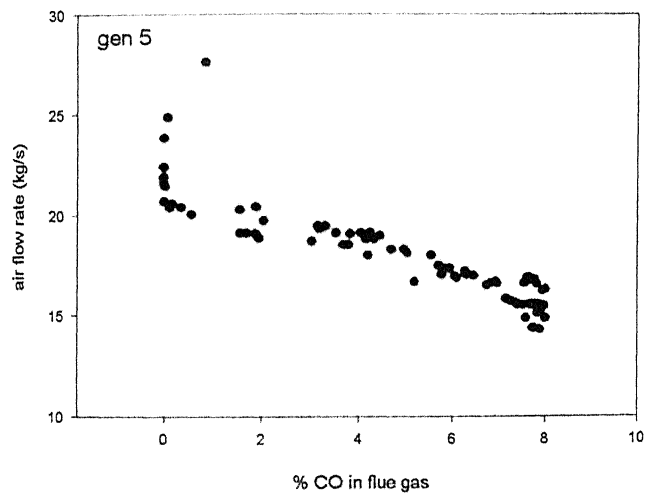
gen 5
air flow rate (kg/s)
% CO in flue gas

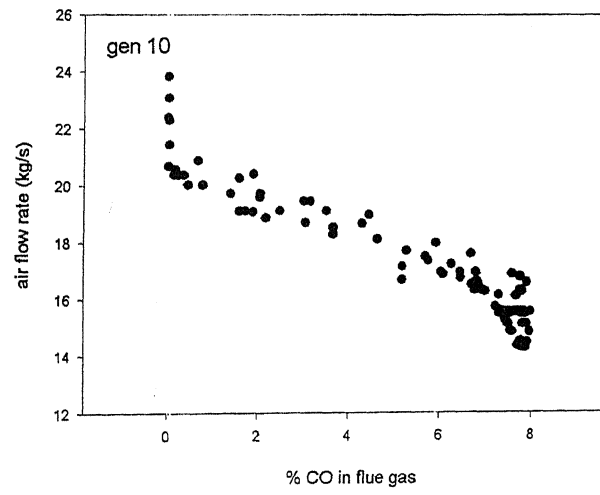
gen 10
air flow rate (kg/s)
% CO in flue gas

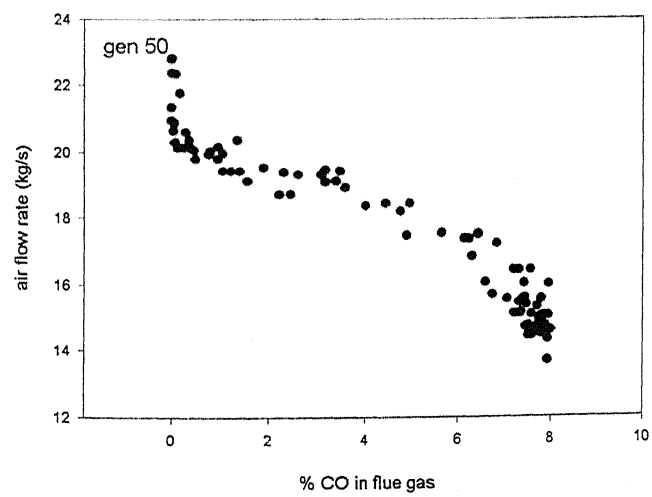
gen 50
air flow rate (kg/s)
% CO in flue gas

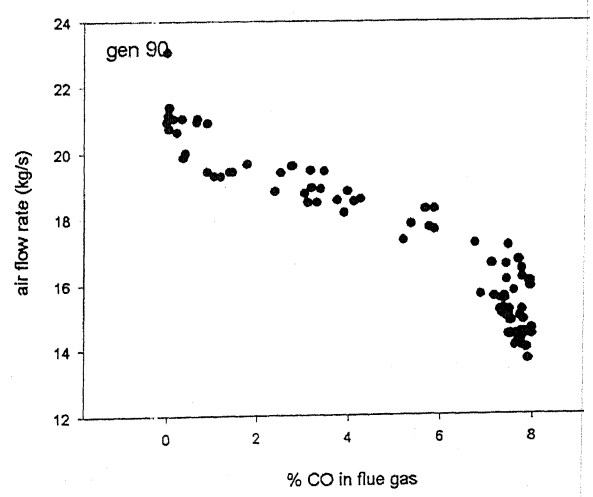
gen 90
air flow rate (kg/s)
% CO in flue gas

Appendix VI

Effect of mutation probability on Pareto set, decision variables and state variables of Problem 4(population size 50; number of generations 50;crossover probability 0

P_m = 0.05 (filled circles); P_m = 0.025 (unfilled circles)

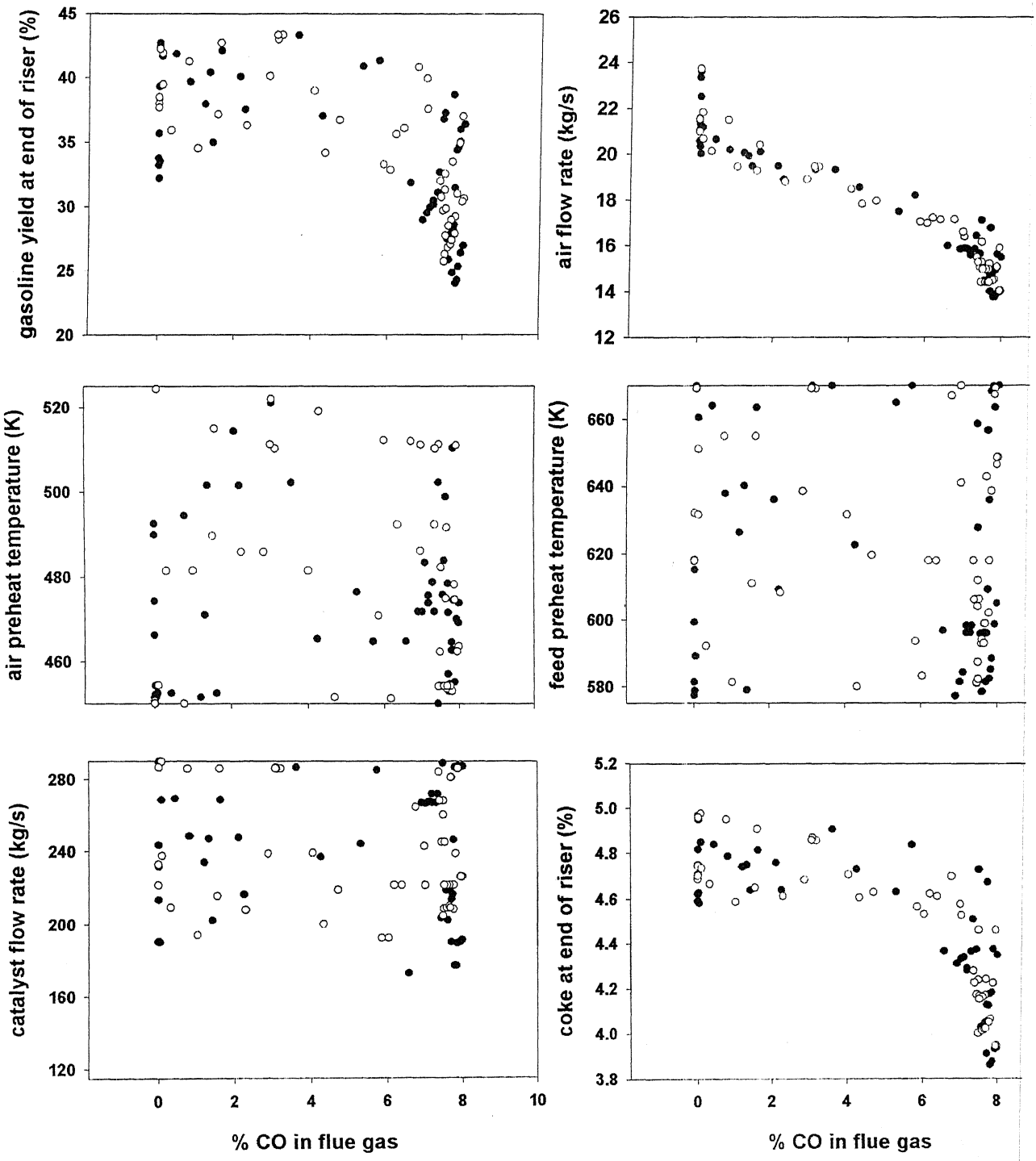

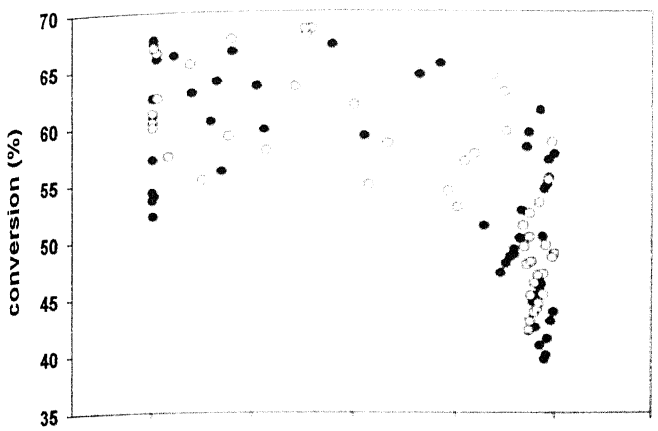
conversion (%)
70
65
60
55
50
45
40
35

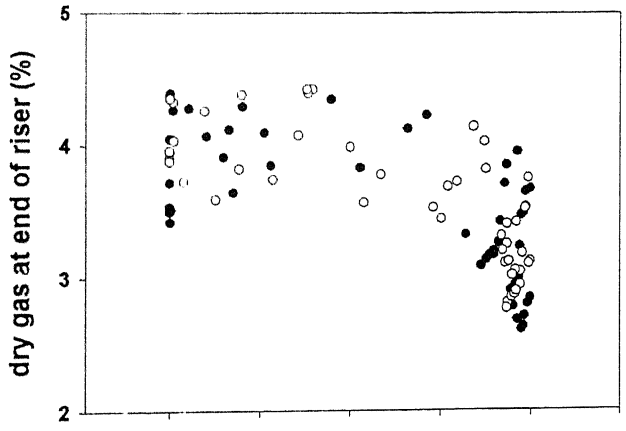
dry gas at end of riser (%)
5
4
3
2

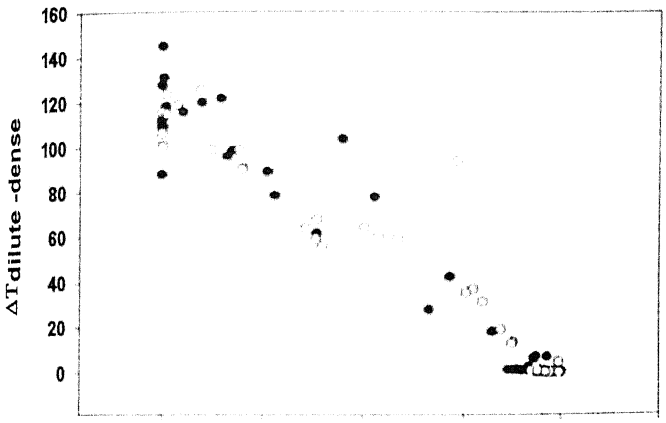
ΔTdilute -dense
160
140
120
100
80
60
40
20
0

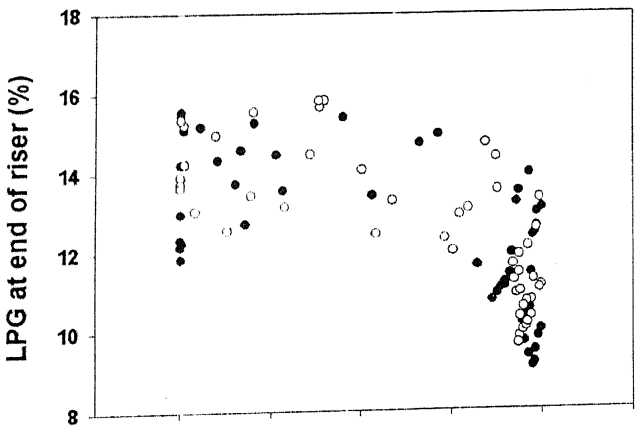
LPG at end of riser (%)
18
16
14
12
10
8

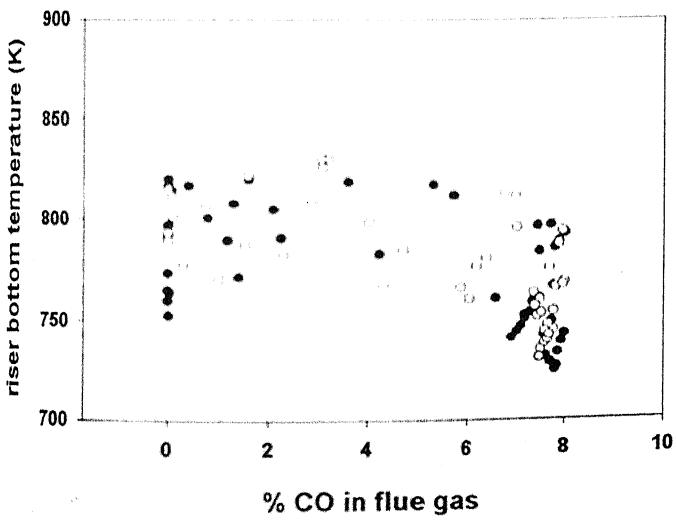
riser bottom temperature (K)
900
850
800
750
700
0
2
4
6
8
10
% CO in flue gas

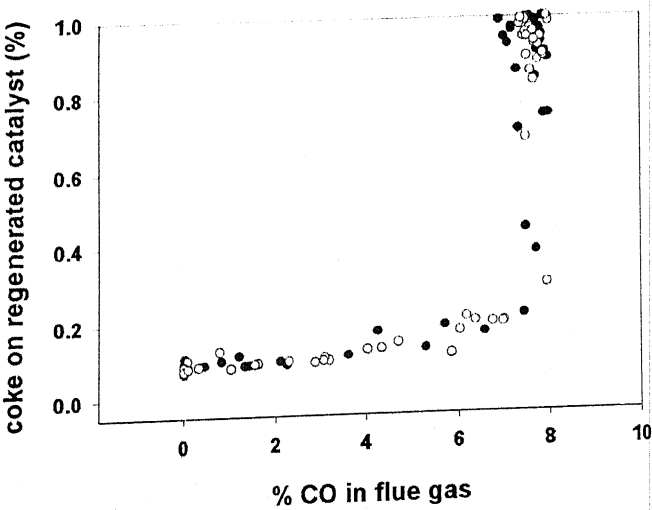
coke on regenerated catalyst (%)
1.0
0.8
0.6
0.4
0.2
0.0
0
2
4
6
8
10
% CO in flue gas

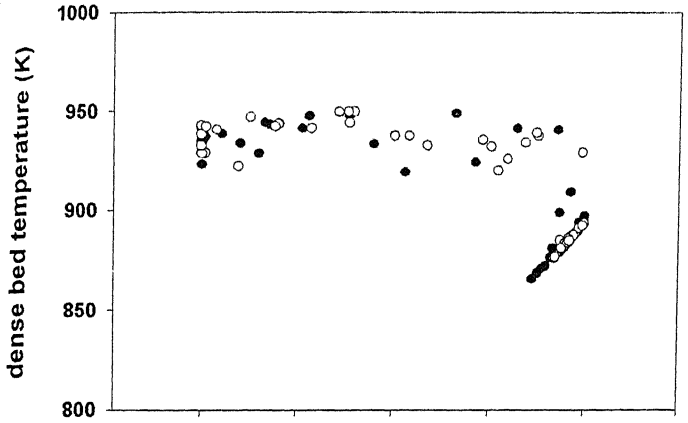
dense bed temperature (K)
1000
950
900
850
800

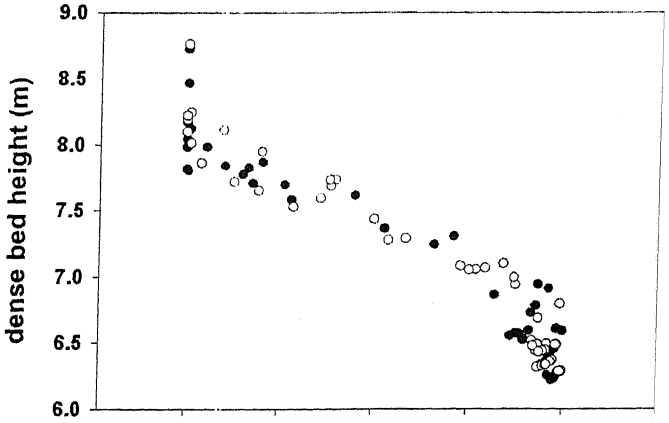
dense bed height (m)
9.0
8.5
8.0
7.5
7.0
6.5
6.0

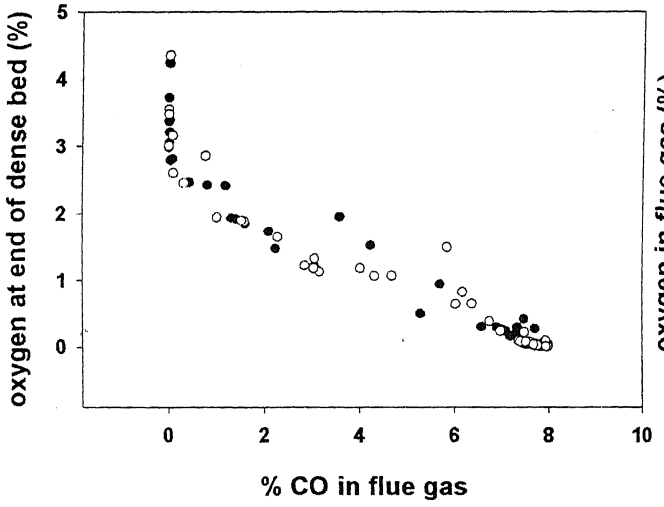
oxygen at end of dense bed (%)
5
4
3
2
1
0
0
2
4
6
8
10
% CO in flue gas

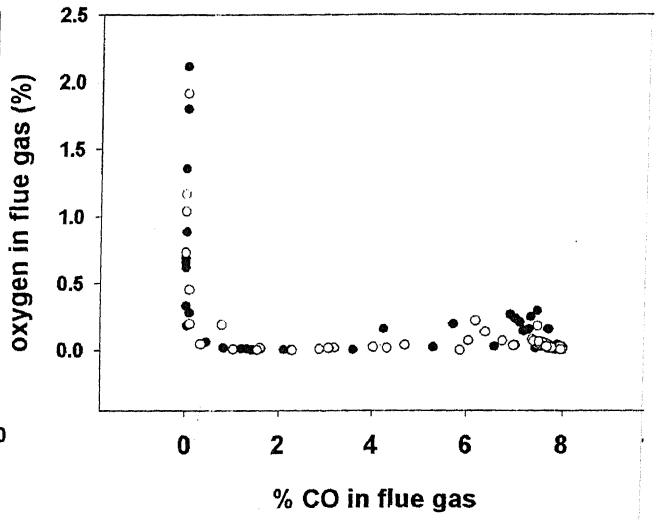
oxygen in flue gas (%)
2.5
2.0
1.5
1.0
0.5
0.0
0
2
4
6
8
% CO in flue gas

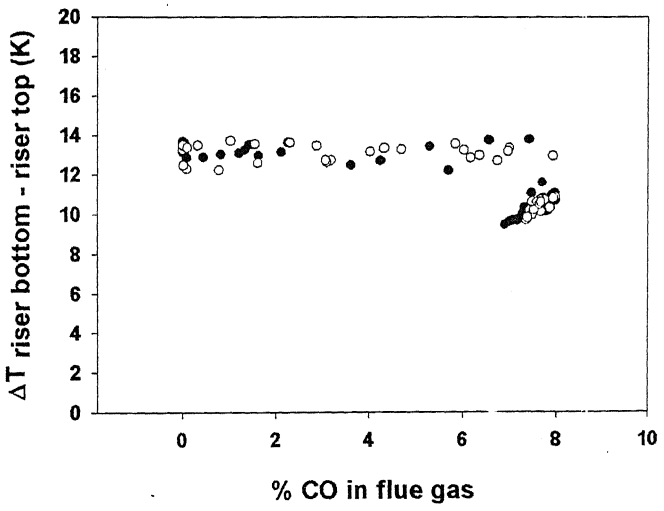
ΔT riser bottom - riser top (K)
20
18
16
14
12
10
8
6
4
2
0
0
2
4
6
8
10
% CO in flue gas

Appendix VII

Effect of crossover probability on Pareto set, decison variables and state variables of Problem 4 (population size 50; number of generations 50; mutation probability 0

P_c = 0.95 (filled circles); P_c = 0.975 (unfilled circles)

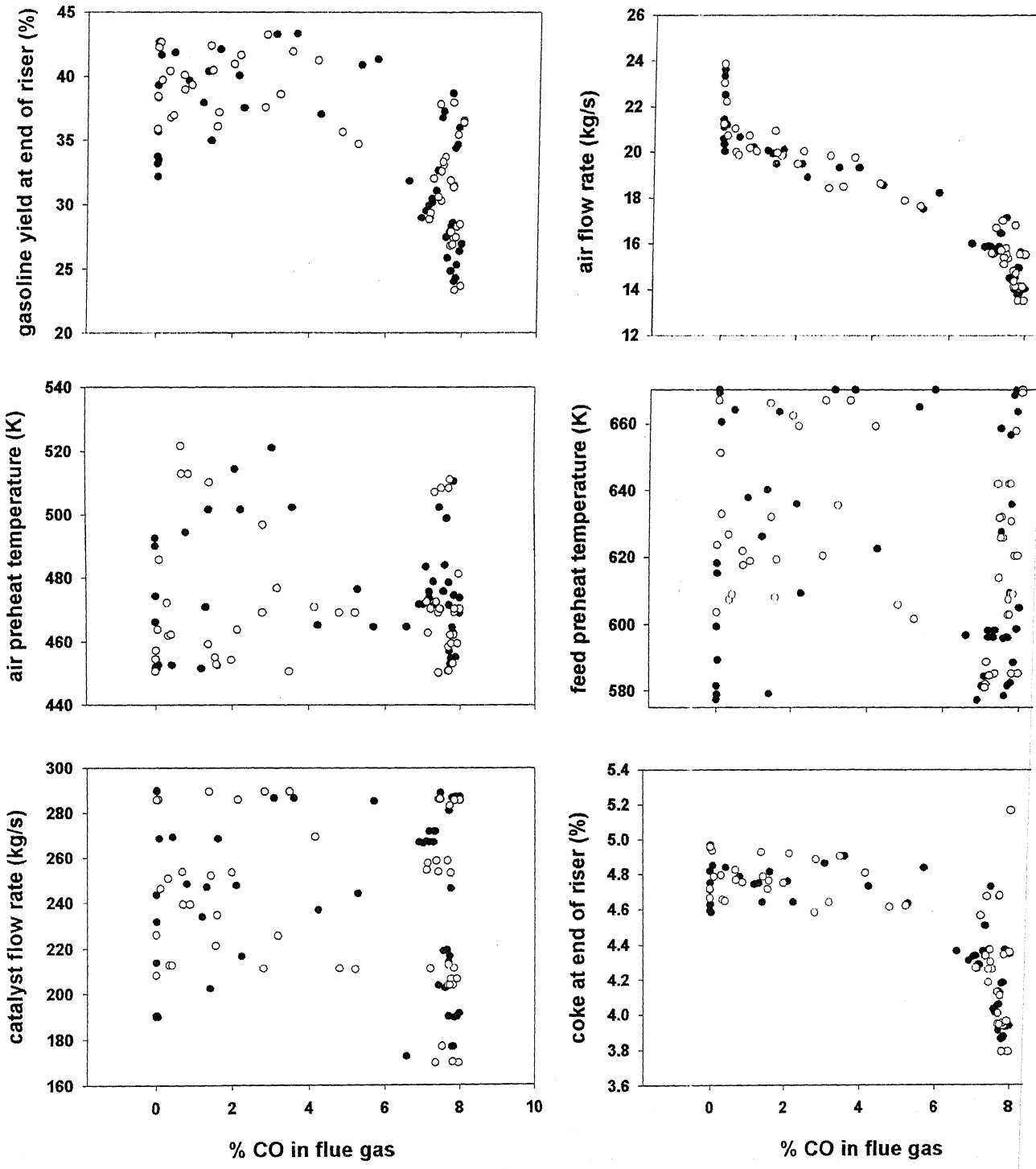

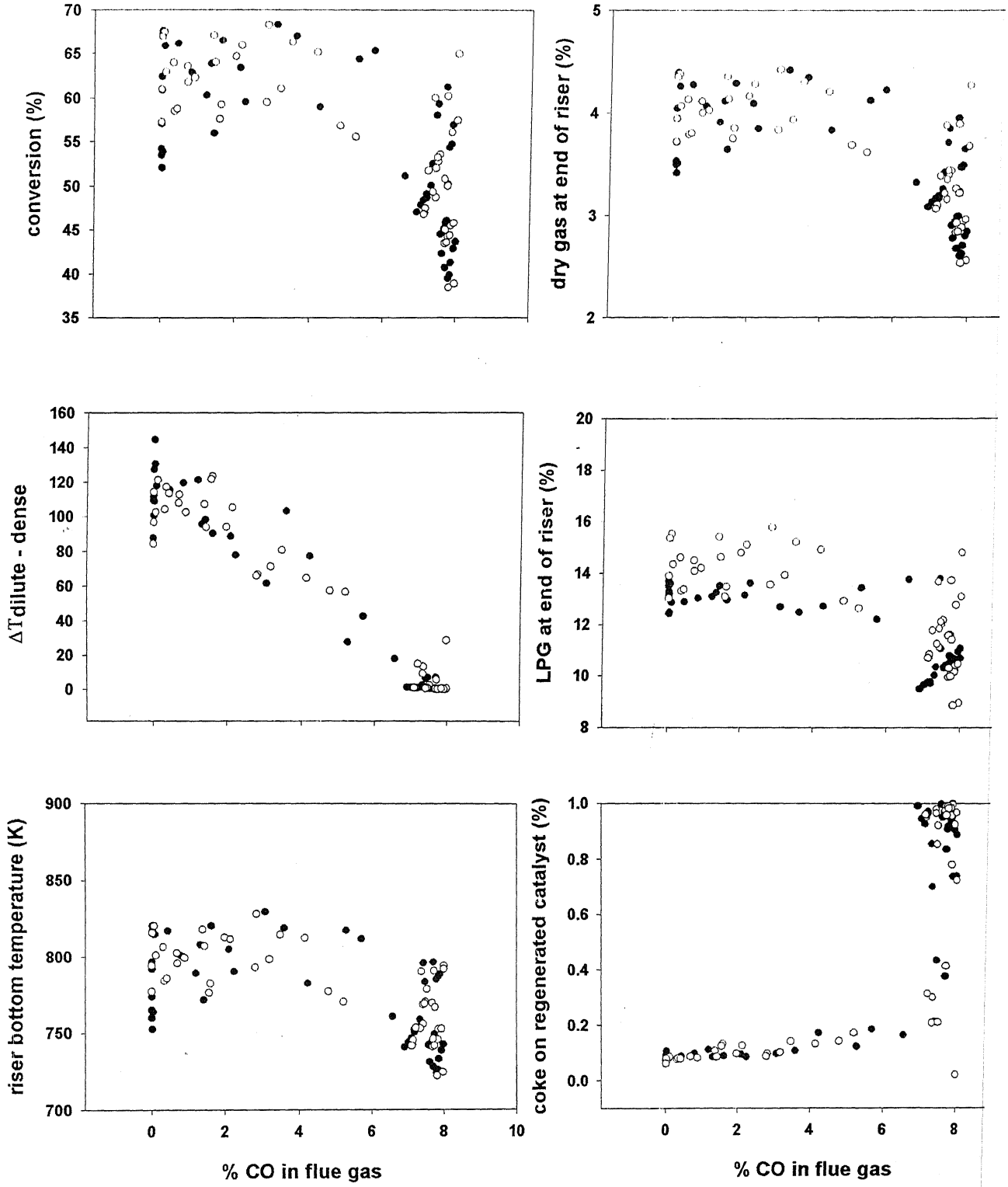
conversion (%)
70
65
60
55
50
45
40
35
dry gas at end of riser (%)
5
4
3
2
ΔTdilute - dense
160
140
120
100
80
60
40
20
0
LPG at end of riser (%)
20
18
16
14
12
10
8
riser bottom temperature (K)
900
850
800
750
700
0
2
4
6
8
10
% CO in flue gas
coke on regenerated catalyst (%)
1.0
0.8
0.6
0.4
0.2
0.0
0
2
4
6
8
% CO in flue gas

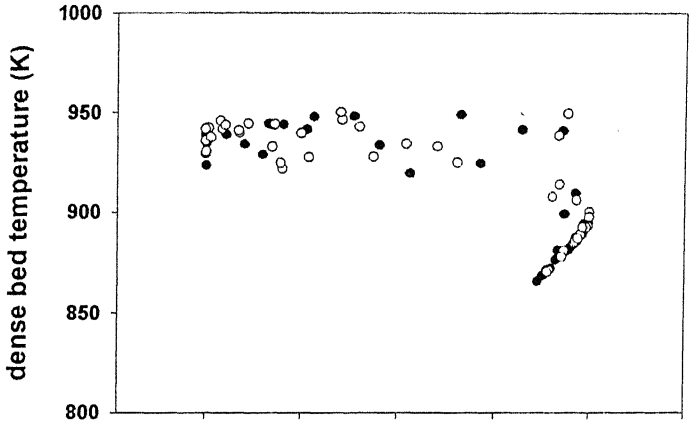
dense bed temperature (K)
1000
950
900
850
800

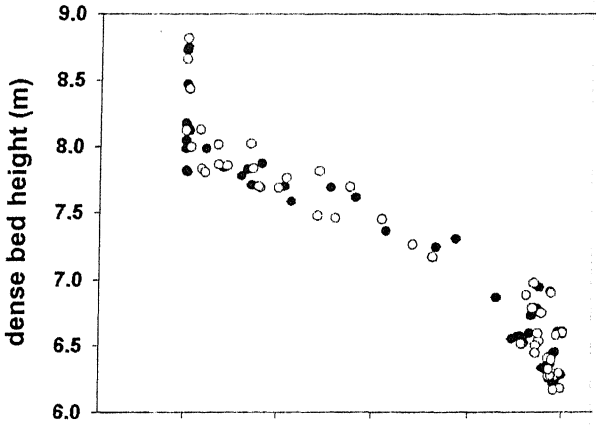
dense bed height (m)
9.0
8.5
8.0
7.5
7.0
6.5
6.0

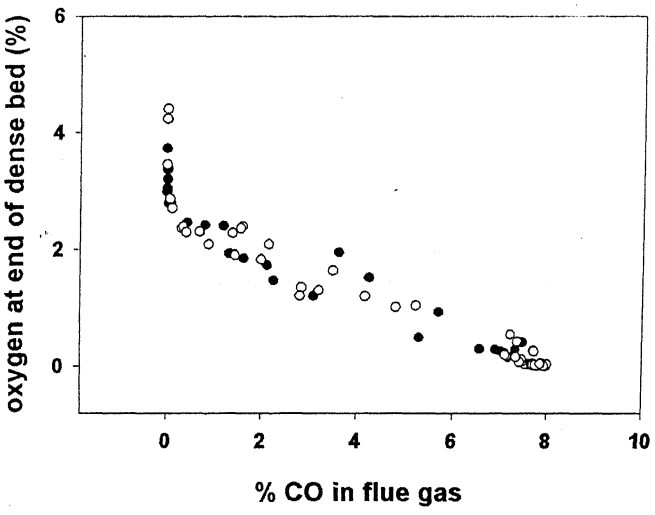
oxygen at end of dense bed (%)
6
4
2
0
0
2
4
6
8
10
% CO in flue gas

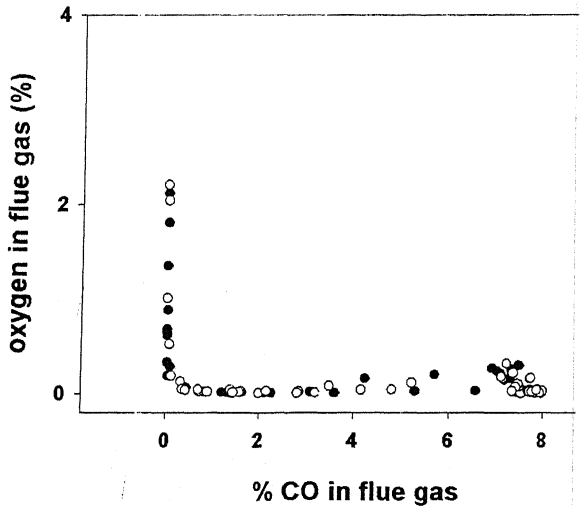
oxygen in flue gas (%)
4
2
0
0
2
4
6
8
% CO in flue gas

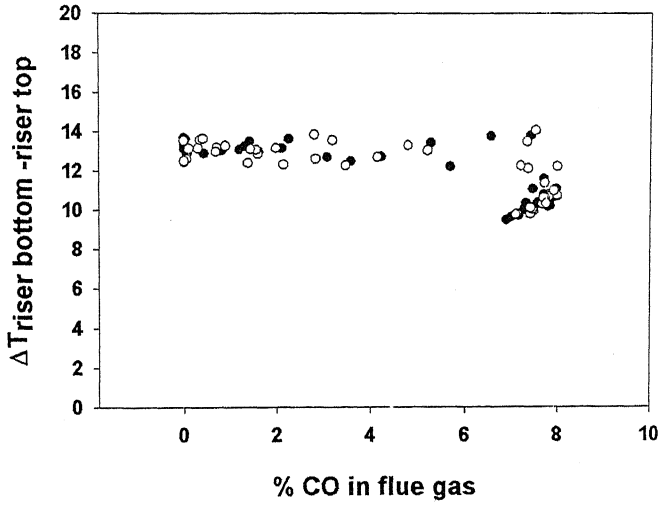
ΔT riser bottom -riser top
20
18
16
14
12
10
8
6
4
2
0
0
2
4
6
8
10
% CO in flue gas